T.C.
IŞIK UNIVERSTIY
SCHOOL OF GRADUATE STUDIES

MASTER THESIS
DEPARTMENT OF ELECTRICAL AND ELECTRONICS ENGINEERING
ELECTRONICS ENGINEERING PROGRAM

Ahmed Hany DALLOUL

ENABLING 5G AND 6G TECHNOLOGIES THROUGH MILLIMETER-WAVE AND VLC INTEGRATION FOR ENHANCED REMOTE HEALTH MONITORING SYSTEMS

SUPERVISOR
Asst. Prof. Farshad MIRAMIRKHANI

İSTANBUL, July 2025

T.C.
IŞIK UNIVERSITY
SCHOOL OF GRADUATE STUDIES

MASTER THESIS
DEPARTMENT OF ELECTRICAL AND ELECTRONICS ENGINEERING
ELECTRONICS ENGINEERING PROGRAM

Ahmed Hany DALLOUL
(22ELEC5002)

ENABLING 5G AND 6G TECHNOLOGIES THROUGH MILLIMETER-WAVE AND VLC INTEGRATION FOR ENHANCED REMOTE HEALTH MONITORING SYSTEMS

SUPERVISOR

Asst. Prof. Farshad MIRAMIRKHANI

İSTANBUL, July 2025

T.C.
IŞIK UNIVERSITY
SCHOOL OF GRADUATE STUDIES

MASTER THESIS
DEPARTMENT OF ELECTRICAL AND ELECTRONICS ENGINEERING
ELECTRONICS ENGINEERING PROGRAM

Ahmed Hany DALLOUL
(22ELEC5002)

ENABLING 5G AND 6G TECHNOLOGIES THROUGH MILLIMETER-WAVE AND VLC INTEGRATION FOR ENHANCED REMOTE HEALTH MONITORING SYSTEMS

Date: 01 / 07 / 2025

Thesis Supervisor: Asst. Prof. Farshad MIRAMIRKHANI / ISIK UNIVERSITY

Jury Members:

Prof. Dr. Onur KAYA/ ISIK UNIVERSITY

Assist. Prof. Sina ALP / ISTANBUL OKAN UNIVERSITY

İSTANBUL, July 2025

ÖZET

5G VE 6G TEKNOLOJİLERİNİN GELİŞİMİ UZAKTAN SAĞLIK İZLEME SİSTEMLERİ İÇİN MİLİMETRE DALGA VE VLC ENTEGRASYONU İLE SAĞLANMASI

Bu tez kablosuz ağların sağlık hizmetlerindeki önemli rolünü incelemekte olup sensörler ve uzaktan izleme ekipmanları gibi tıbbi cihazlar arasında verimli veri aktarımını sağlamak için 5G ve gelişmekte olan 6G gibi yüksek performanslı teknolojilere duyulan ihtiyacı vurgulamaktadır. Uzaktan sağlık izleme sistemlerinde 5G mmWave teknolojisinin mevcut araştırma alanını ele alarak, uygulamaları, ana zorlukları ve gelecekteki eğilimlere odaklanıyoruz. Yeniden yapılandırılabilir hibrit optik-radyo tabanlı Tıbbi Vücut Sensör Ağlarının (MBSN'ler) kablosuz bağlantı gereksinimlerini inceleyerek, geleneksel MBSN'lerin daha esnek ve genel çözümlere genişletilmesini öneriyoruz.

Bu tez, anten tasarımı, küçük implante edilebilir antenler, vücut üzerinde giyilebilir çözümler ve uyarlanabilir algılama ve görüntüleme sistemleri gibi çeşitli alanlarda kapsamlı bir literatür taraması sunmaktadır. Araştırmamız ayrıca izleme sistemlerindeki metodolojik yaklaşımları, kanal karakteristiklerini analiz ederek kablosuz kapsül endoskopisindeki ilerlemeleri ve algılama ve görüntüleme tekniklerini incelemektedir.

Ayrıca 6G çerçevesinin sağlık hizmetlerinde Görünür Işık İletişimini (VLC) nasıl entegre ettiğini araştırarak, VLC tabanlı MBSN'lerin uzaktan hasta izleme ve gerçek zamanlı sağlık verisi iletimini kanal DC kazancı ve RMS gecikme yayılımı gibi VLC kanal parametrelerini doğru bir şekilde tahmin ederek nasıl devrim yaratabileceğini göstermekteyiz.

Farklı hastane ortamlarında (yoğun bakım ünitesi ve aile tipi hasta odası gibi) kanalları modellemek, yol kaybı ve RMS gecikme yayılımını tahmin etmek

için gelişmiş bir ışın izleme tekniği ve ML tabanlı bir algoritma tanıtıyoruz. Hastane senaryolarının detaylı sonuçları, LSTM, GRU, RNN, Linear Regression SVR ve KNN gibi çeşitli makine öğrenimi algoritmaları kullanılarak listelenmiştir. Tahminler, en iyi performans gösteren ML tekniği seçilerek kapsamlı bir şekilde detaylandırılmış ve açıklanmıştır.

Anahtar Kelimeler: Uzaktan Sağlık İzleme, 6G, VLC Tabanlı MBSN'ler, Yol Kaybı Ve RMS Gecikme Yayılımı, Makine Öğrenimi

ABSTRACT

ENABLING 5G AND 6G TECHNOLOGIES THROUGH MILLIMETER-WAVE AND VLC INTEGRATION FOR ENHANCED REMOTE HEALTH MONITORING SYSTEMS

This thesis examines the pivotal role of wireless networks in healthcare, emphasizing the need for high-performance technologies like 5G and emerging 6G to enable efficient data transfer between medical devices such as sensors and remote monitoring equipment. We delve into the current research landscape surrounding 5G mmWave technology in remote health monitoring systems, focusing on its applications, main challenges, and future trends. We explore the wireless connectivity requirements of reconfigurable hybrid optical-radio-based Medical Body Sensor Networks (MBSNs), proposing an extension of conventional MBSNs to more flexible and generic solutions.

This thesis introduces a comprehensive literature review across diverse domains including antenna design, small implantable antennas, on-body wearable solutions, and adaptable detection and imaging systems. Our research further investigates methodological approaches in monitoring systems, analyzing channel characteristics, advancements in wireless capsule endoscopy, and sensing and imaging techniques.

Additionally, we explore how 6G's framework integrates Visible Light Communication (VLC) in healthcare, demonstrating how VLC-enabled MBSNs can revolutionize remote patient monitoring and real-time health data transmission by accurately estimating VLC channel parameters, such as channel DC gain and RMS delay spread.

We introduce a sophisticated ray tracing technique and ML-based algorithm to model channels and estimate path loss and RMS delay spread within different hospital settings such as ICU ward and family-type patient room. The

detailed results of the hospital scenarios are listed using various machine learning algorithms such as LSTM, GRU, RNN, Linear Regression SVR, and KNN. The estimation was illustrated and detailed comprehensively by choosing the best-performing ML technique.

Keywords: Remote Health Monitoring, 6G, VLC-Based MBSNs, Path Loss And RMS Delay Spread, Machine Learning

ACKNOWLEDGEMENT

I want to express my sincere gratitude to my supervisor, Asst. Prof. Farshad Miramirkhani, for supporting me throughout my master's degree journey. His guidance and belief in me were remarkable in helping me achieve this work. It was an honor to work under such a great professor.

I would also like to extend my heartfelt thanks to Prof. Dr. Onur Kaya, who had the most significant impact on me during my academic journey.

Many thanks to the committee members for their time and effort spent in all aspects of this work.

Lastly, I would like to thank my parents and friends for their unconditional support, true belief in me, and encouragement to achieve my studies and become a better person each day. I am honored to have them in my life.

Ahmed Hany DALLOUL

TABLE OF CONTENTS

LIST OF FIGURES

LIST OF TABLES

ABBREVIATIONS LIST

ADC: Analog-to-Digital Converter

AI: Artificial Intelligence

AM: Amplitude Modulated

AS: Amplitude Sensitivity

BAN: Body Antenna Network

BBU: Baseband Unit

BER: Bit Error Rate

B5G: Beyond Fifth Generation of Mobile Networks

CGRS: Confocal Gregorian Reflector System

CIR: Channel Impulse Response

CP: Circularly Polarized

CPRI: Common Public Radio Interface

CW: Continuous Wave

DA: Detection Accuracy

DDR: Dielectric Disc Resonator

DIG: Dielectric Image Waveguide

DL: Detection Limit

DMA: Dynamic Metasurface Antennas

EM: Electromagnetic

eMBB: Enhanced Mobile Broadband

EOP: Eye Opening Penalty

EVM: Error Vector Magnitude

FEM: Finite Element Method

5G: Fifth Generation of Mobile Networks

FM : Frequency Modulated

FoM: Figure of Merits

FSK: Frequency Shift Keying

FTPR: Family-Type Patient Rooms

FTTD: Finite Difference Time Domain

GBSM: Geometry Based Stochastic Model

GMS: Gradient Metasurface

GRU: Gated Recurrent Units

GST: Ge2Sb2Te5 Material

HBC: Human Body Communication

HPBW: Half-power Ray Width

ICU: Intensive Care Unit

IM-DD: Intensity Modulation Direct Detection

IoMT-based WBAN: Internet of Medical Things-based Wireless Body Area Network

IoT: Internet of Things

ISI: Intersymbol Interference

ISM: Industrial, Scientific, and Medical

KNN: K-Nearest Neighbors

LED: Light Emitting Diode

LoS: Line of Sight

LP: Linear Polarization

LSTM: Long Short-Term Memory

LWA: Leaky-Wave Antenna

MAE: Mean Absolute Error

MAPE: Mean Absolute Percentage Error

MBSNs: Medical Body Sensor Networks

MFH: Mobile Fronthaul

MIMO: Multiple-Input Multiple-Output

ML: Machine Learning

mMTC: Massive Machine-Type Communications

mm-Wave: Millimeter Wave

MRI: Magnetic Resonance Imaging

MSE: Mean Squared Error

NIR: Near Infrared

NP: Nanoparticle

OBI: Optical Brain Imaging

OFDM: Orthogonal Frequency Division Multiplexing

OOK: On-off Keying

PCF: Photonic Crystal Fiber

PCR: Polarization Conversion Rate

PDs: Photodetectors

PDMS: Polydimethylsiloxane

PLL: Phase-locked Loops

PPM: Pulse-Position Modulation

QPSK: Quadrature Phase Shift Keying

RF: Radio Frequency

RI: Refractive Index

RMS: Root Mean Square

RMSE: Root Mean Squared Error

RNN: Recurrent Neural Network

RRU: Remote Radio Unit

RS: Reed Solomon

6G: Sixth Generation of Mobile Networks

SAR: Specific Absorption Rate

SNR: Signal-to-Noise Ratio

SoC: Interface System-on-Chip

SP: Surface Plasmon

SPR: Surface Plasmon Resonance

SSPs: Spoof Surface Plasmon Polaritons

SVR: Support Vector Regression

TDM: Time Division Multiplexing

TF/SF: Total Field/Scattered Field

THz: Terahertz

ToA: Time of Arrival

URLLC: Ultra-Reliable Low Latency Communications

UWB: Ultra Wideband

VLC: Visible Light Communication

VSWR: Voltage Standing-wave Ratio

WCE: Wireless Capsule Endoscope

WGM: Whispering-gallery-mode

WLAN: Wireless Local Area Network

WMTS: Wireless Medical Telemetry Service

WS: Wavelength Sensitivity

WSNs: Wireless Sensor Networks

CHAPTER 1

1. INTRODUCTION

Remote health monitoring, also known as telehealth or remote patient monitoring, utilizes technology to monitor the health of individuals remotely. The use of such technology enables medical professionals to track patients, deliver timely interventions, and make informed decisions by collecting, transmitting, and analyzing health data (Yakovlev et al., 2012). Various technologies such as communication networks, mobile applications, along with wearable sensors and devices have been developed to support this monitoring (Marzencki et al., 2011; Mia et al., 2021; Ramesh et al., 2012). Implementing remote health monitoring systems has shown significant potential for enhancing patient outcomes, improving obedience to the medication, as well as increasing engagement and satisfaction. These systems offer personalized treatment, facilitate distant consultations, and promote self-care for medical conditions (Hassan et al., 2013). Figure 1.1 illustrates the overall architecture of these systems. The main objectives here are twofold: first, to improve connectivity within the body which results in enhancing the imaging and detecting systems functionality for early identification such as cancer or glucose levels; second, in order to improve implantable sensors and antennae implemented within various devices, such as wireless capsule endoscopes and MRI imaging gadgets. It's important to highlight that Tier 1 focuses on gathering vital signs data from interoperable wearable medical devices, which then transmit it to Tier 2. Our primary emphasis here is on the advancements within this initial tier.

Remote health monitoring systems face huge concerns such as data security, reliability, and power consumption (Boric-Lubecke et al., 2014; Petković, 2009; Sagahyroon, 2017). A critical issue is securing sensitive medical data during wireless transmitting, which is vulnerable to cyber-attacks. Reliability is essential, as system failures can result in delayed interventions or incorrect

diagnoses. Another concern is the wearable devices' power consumption which forms an issue for patients who utilize devices on batteries that require frequent charging. Further investigation is necessary to tackle these obstacles and maximize the use of diverse technologies in healthcare for improved results (Bhatti et al., 2018).

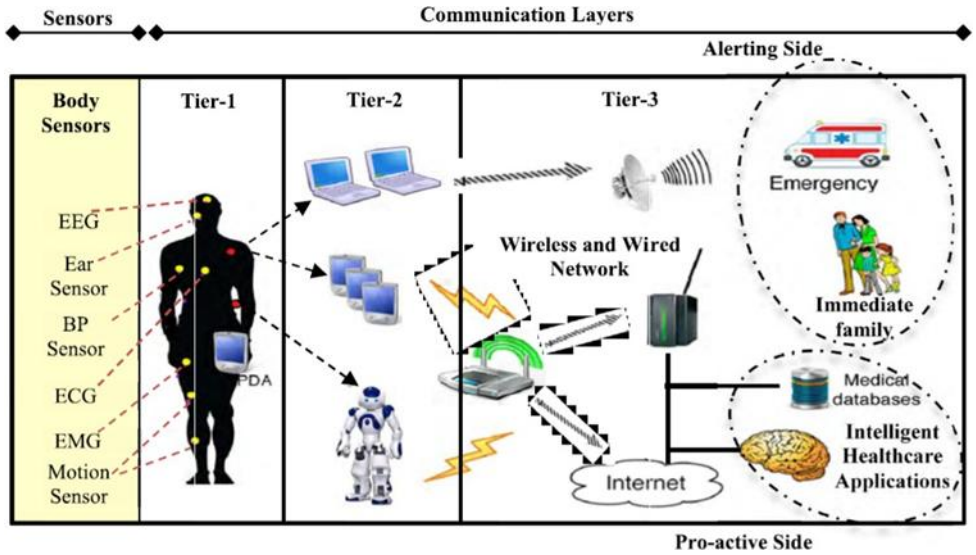

Figure 1.1: The remote health monitoring system's infrastructure (Albahri et al., 2019)

Moreover, several studies (Boyle, 2006; Ishida et al., 2020; Periyasam & Dhanasekaran, 2013) have explored some of the concerns like the electromagnetic compatibility and safety in the interface among medical devices and wireless networks. Furthermore and according to international standards (Boyle, 2006) it highlights that devices of mutual interference like cell phones, have the biggest risk, while networks in local areas that present minimal interference have no risk. Therefore, wireless technologies can be used safely when maintaining recommended separation distances from medical devices. Additionally, (Ishida et al., 2020) examined noisy lighting interference caused by electromagnetic in wireless medical telemetry and proposed solutions. Another study by (Kuila et

al., 2023) suggests that carbonaceous materials can serve as electromagnetic shielding to reduce the impact of electromagnetic pollution on wearable devices.

This thesis provides a thorough overview of the latest advancements within remote patient monitoring device development. It also highlights previous studies, focusing on their key areas, relevance, and how they address gaps in the literature (See Table 1.1). Our review research is divided into two parts. The first part concentrates on developments in remote health monitoring devices, exploring various antenna models implemented for patient monitoring, their diversity, and scenarios. We also delve into compact in-body implantable antennae for critical usage and wearable antennas for on-body applications. Additionally, we examine detection and imaging systems, showcasing their wide range of applications within health monitoring.

The second part of the review research delves into the methodologies employed in remote health monitoring systems, providing an in-depth look at various approaches, including channel characterization studies across diverse devices. It also highlights advancements in wireless capsule endoscopy (WCE), underscoring its significance in remote health monitoring. The part concludes by focusing on sensing and imaging techniques, offering a thorough overview of the tools and technologies driving progress in this domain.

The rest of the thesis is organized as follows: Chapter 2 offers a detailed review of recent advancements in remote health monitoring devices within section 2.1, while section 2.2 focuses on the current approaches and methods employed in this domain. Chapter 3 outlines the system model and problem formulation of VLC-based MBSNs, Also, it delves into the application of machine learning approaches for estimation of channel parameters and presents the detailed results of such techniques. Chapter 4 discusses potential future developments in remote health monitoring systems. Lastly, Chapter 5 summarizes the findings and conclusions based on the work done throughout the dissertation.

Table 1.1: Overview of recent surveys on remote health monitoring (Dalloul et al., 2023).

Ref.	Year	Surveys Content details
(Buke et al., 2015)	2015	Examined three healthcare algorithm applications utilizing wearable inertial sensors
(Kocabas et al., 2016)	2016	Assessed various encryption techniques to ensure data security in medical cyber-physical systems
(K et al., 2016)	2016	Analyzed existing remote patient monitoring systems used to measure different physiological parameters
(King & Sarrafzadeh, 2018)	2017	Reviewed remote health monitoring applications designed for smartwatches
(Gabor & Gausz, 2018)	2018	Presented low-power and bandwidth-e□icient sensor designs for remote health monitoring
(Usman et al., 2018)	2018	Suggested a four-tier security framework and reviewed research aimed at improving wireless body area network security and privacy
(Mshali et al., 2018)	2018	Summarized health monitoring solutions for smart homes catering to dependent and elderly individuals
(Gahlot et al., 2019)	2019	Discussed and analyzed various smart health monitoring technologies
(Wang et al., 2021)	2021	Reviewed the application of the global navigation satellite system for bridge structural health monitoring
(Shah et al., 2021)	2021	Presented a remote health monitoring solution to reduce clinical workload during the COVID pandemic
(P. Ma et al., 2022)	2022	Analyzed multitemporal interferometric synthetic aperture radar used for infrastructure health monitoring
(Oh et al., 2022)	2022	Explored the advantages of continuous remote patient monitoring for COVID-19 patients to reduce emergency department readmissions
(Ashok& Gopikrishnan,2023)	2023	Surveyed IoT remote health monitoring security techniques using different methods
(Junior et al., 2023)	2023	Reviewed different resource-e□icient systematic remote pedestrian localization systems

Table 1.1: (Continue) Overview of recent surveys on remote health monitoring (Dalloul et al., 2023).

(Krishna et al., 2023)	2023	Analyzed research on remote health monitoring systems for pandemic patients
(Abdellatif et al., 2023)	2023	Reviewed recent advancements in reinforcement learning techniques for intelligent healthcare systems
This survey	2023	Provided a comprehensive analysis of various antenna architectures within patient monitoring applications, small in- body implantable antennas, wearable antenna designs for on- body applications, detection and imaging systems, channel properties between devices, advancements in wireless capsule endoscopy (WCE), together with sensor and imaging technology system methods.

CHAPTER 2

2. LITERATURE SURVEY

2.1 ADVANCEMENTS IN REMOTE HEALTH MONITORING DEVICES

Technologies for the fifth generation and beyond (5G/B5G) have progressed to a point where they can provide dependable connectivity, minimal latency, and high-speed data transfer. This development unlocks new opportunities for telehealth. Lately, such innovations served a significant part in assisting the elderly population by enabling early detection through the use of health monitoring devices. We presented the idea of patient remote monitoring in the previous section, reviewing its advantages and di□iculties. In this section, we will present an in-depth review of the newest developments in the innovation field of devices. Some studies introduced different antenna schemes utilized in various patient monitoring applications, while others focus on small implanted antennas for essential usage within bodies and different motivations. Additionally, on-body wearable antenna designs, particularly for detection and imaging systems, are also discussed.

It is important to point out that this section offers in-depth details about the improvements in features of various devices and the general influence of these advances on the industry. The discussion may cover newly introduced technologies, innovative features, and enhancements within e□iciency, performance, and experience of users. However, Section 2.2 concentrates on implemented techniques explaining surveillance networks employed in this area.

This section describes approaches, strategies, and practices employed within underlying systems. While Section 2.1 addresses the advancements in device development, Section 2.2 enhances on these developments by emphasizing the techniques and approaches implemented for surveillance

networks that take advantage of these advances. Collectively, both sections present complete recent device technology developments grasped together with their application in surveillance systems. This helps readers to better grasp the field's present status as well as the methods used to collect and evaluate data.

Dynamic metasurface antennas (DMAs), which offer simplicity and an effective range, are employed in (Oesterling et al., 2020) for radio frequency (RF) sensing motion applications in residential settings. Moreover, the suggested DMA can detect minute movements, i.e., individual micro movements breath within a line of sight (LoS) or non-line of sight (NLoS) manner, and generate several reconfigurable patterns at a single frequency. Furthermore, the DMA proposal takes into account the single noise calibration floor and can be implemented within various room structures, making it a possible hardware option for seamless monitoring of patients and intruder detection.

Additionally, (Li et al., 2020) introduce another metasurface antenna design applied to optical sensing for telehealth systems. In this design, the phase-changing $Ge_2Sb_2Te_5$ (GST) material which is recognized for its high conversion rate and exceptional transmittance e□iciency is utilized in an active rectangular wave plate antenna metasurface. With a quarter-wave plate, the first metasurface functions at a wavelength of 10.0–11.9 μm. On the other hand, the half-wave plate metasurface of GST functions at a wavelength of 10.3–10.9 μm when it is in its crystalline state. Figure 2.1 illustrates the two-wave plate metasurface. The design achieves a 99.9% polarization conversion rate (PCR) and improved transmittance e□iciency by using both electric and magnetic resonance dipoles.

Moreover, (Yan et al., 2022) explore a different antenna design that uses a grooved metal antenna to stimulate spoof surface plasmon polaritons (SSPs) using a 1D dielectric gradient metasurface (GMS) coupler. This design's performance in the THz region was also evaluated. Unlike conventional metal antennas, the proposed SSP antenna minimizes loss of absorption and great efficiency sub-wavelength. The compact and ultrathin design of the SSP enables its use in wireless health monitoring applications.

The findings show that the 0.46 THz-resonating SSP GMS offers 517.9 GHz/RIU high sensitivity, 262 high Q-factor, and a resolution of 0.0001 RIU. Further investigation shows that the refractive index may be detected with 410 GHz/RIU sensitivity and 0.05 RIU resolution.

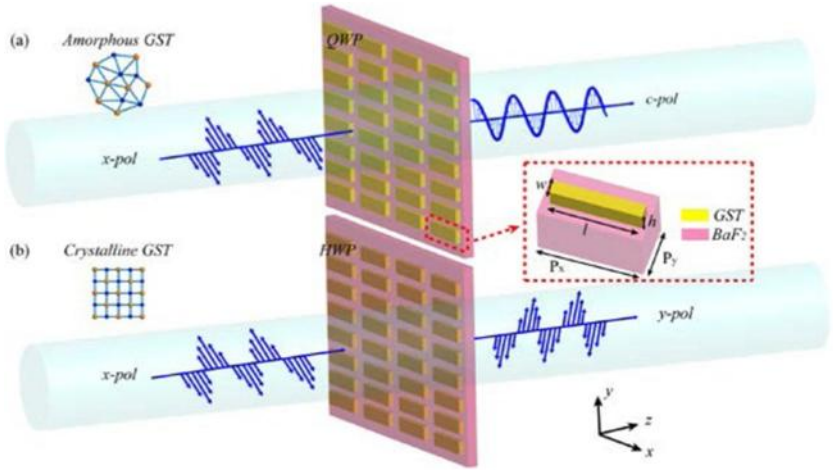

Figure 2.1: Rectangular metasurface antenna including two types of plates a) Quarter-wave plate in amorphous GST state and b) Half-wave plate in crystalline GST state (Li et al., 2020)

Moreover, (Čibiraitė-Lukenskienė et al., 2020) present a different antenna approach. The work presents passive imaging with a broadband uncooled detector, utilizing human body radiation within the range of lower THz frequency. Figure 2.2 illustrates the detector design that combines a log-spiral THz antenna with a Si CMOS field-effect transistor. According to experimental data, responsiveness is constant between 0.1 and 1.5 THz frequency range. The sensor attains a noise-equivalent power of 42 pW/√Hz with an optical responsivity of 40 mA/W. These results are consistent with simulations pointing to a wider responsivity range than 2.0 THz. Additionally, an image of a hand's fingers, measuring 2.3 x 7.5 cm^2 with 1 mm^2pixel size and 1 mm/s scanning speed was obtained. The results showed a noise-equivalent temperature difference of 4.4 and an SNR ratio of 2, which indicates good image quality.

Hence and for THz frequency detection applications, this architecture is suitable for remote health monitoring systems.

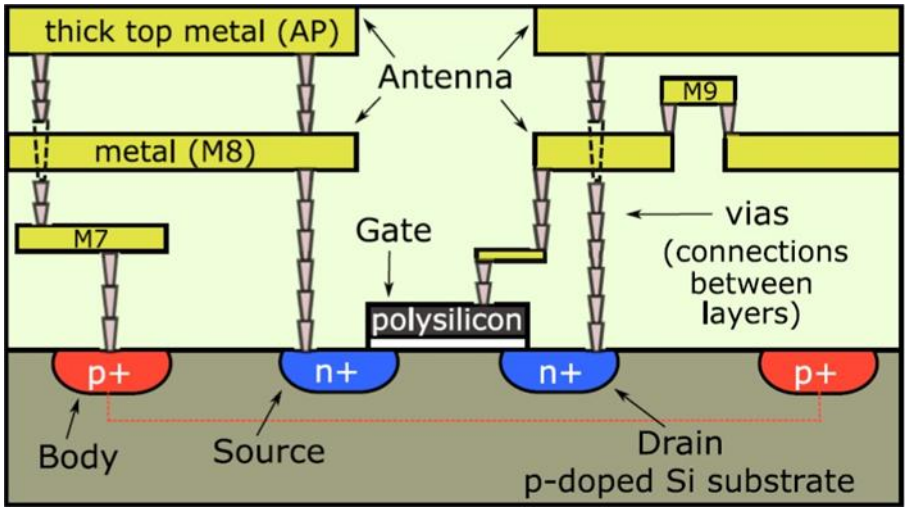

Figure 2.2: The log-spiral antenna integrated within the chip (Čibiraitė Lukenskienė et al., 2020)

The wideband spiral antenna design discussed in (Lee et al., 2011) is intended for ingestible capsule endoscope systems, which are utilized for imaging and detection in surveillance monitoring. Additionally, experiments comparing the design's performance in humans and an anesthetized pig are presented. Using on-off keying (OOK) modulation, the capsule uses a small-sized antenna to provide high-resolution, real-time images to the receiver. An isotropic radiation pattern is produced by the antenna inside the capsule to enable image transmission independent of the position of the capsule. In addition, the effectiveness of the antenna was confirmed by measuring received power and return loss in an anesthetized pig using a circularly polarized antenna; the results were comparable to those obtained with a human phantom.

Another UWB symmetrical two-loop antenna design working within the ISM band is shown in (Shang & Yu, 2019). The antenna design consists of dual identical loops with parasitic and feeding patches in the middle. Based on simulation results, it is possible to attain 143% UWB within the ISM band

spanning between 1.11 and 6.03 GHz by using dual rectangular patches together with a 90° feeding direction angle. The developed antenna results with 124% bandwidth when demonstrated on pork which represents suitability for different biomedical applications such as ingestible wireless endoscopy.

The antenna-in-package design in (Chu et al., 2019) uses Bluetooth technology on a smartphone that allows data transfer between wireless ingestible capsules operating inside the ISM band. A modified inverted-F design is included in the antenna structure to create polarization variety while reducing size. Performance analysis demonstrates that, regardless of the orientation of the capsule, the design offers strong link margins and digestive organs immunity along with reflection measurements of the antenna utilizing a phantom of muscle-mimicking.

The wideband implantable antenna with capacitance load used in (Cui et al., 2019), is in favor of utilization for wireless capsule endoscopy (WCE) architecture. The antenna's ground plane and radiator are carved to minimize bulk and enhance bandwidth impedance. Impedance matching can also be optimized by including capacitance loading. This design outperforms previous models in the pattern of radiation, bandwidth of impedance, and specific absorption rate (SAR), according to experimental tests on chicken breasts. The antenna occupies only 120 mm^3 compact volume and the projected impedance bandwidth spans from 2.17 to 2.69 GHz, with 20.5% for |S11| less than -10 dB bandwidth.

Furthermore, a 434 MHz ultraminiature low-profile wireless in-body antenna intended for ingestible and implantable applications in telemedicine tracking is presented in (Nikolayev et al., 2017). The antenna is down sized using an analytical method that avoids impedance detuning, and the system functions with an input impedance of 50 Ω. A biocompatible capsule's interior surface is also improved. To ensure increased resilience, the antenna's performance is tested in heterogeneous phantoms that replicate the tissue of the gastrointestinal tract using a high-permittivity capsule. Considering the radiation and reflection coe□icients, the measurement results demonstrate consistent performance.

The paper (Xu et al., 2020) introduces a circularly polarized antenna for wireless embedded applications within the ISM band for monitoring patients remotely. The antenna's input impedance is examined in conjunction with a minimized ground in lossy muscle tissue. To improve impedance matching, arc-shaped slots, shorting pins, and LC components are included. The simulations show an axial ratio, 18.3% circular polarization bandwidth, and satisfactory impedance matching for the $\pi * 4.82$ small antenna.

Moreover, a highly directed embedded dipole antenna with linear polarization is shown in (Aggarwal et al., 2017) for 60 GHz millimeter-wave radio. In order to decrease the interference of channels within wireless links, the system employs the use of 1.5 T MRI together with time division multiplexing (TDM) and modulation of on-off keying (OOK). A raw bit error rate (BER) of 10^{-6} is reached across 10 cm, which is better than 10^{-2} BER for WiFi or 802.11n systems as well as 10^{-3} BER Bluetooth Thus, wearable wireless MRI receivers in remote healthcare applications could benefit from this topology.

In addition, circularly polarized (CP) based antenna design within the band of ISM is presented in (Xu, Jin, et al., 2020) for remote health monitoring systems that diagnose and monitor physiological parameters. A pin-loaded patch with two non-degenerated orthogonal modes and two open-ended slots is integrated into the antenna design. Moreover, in lossy tissues, the walls around the pin-loaded patch serve to reduce gain loss. Simulations show an impedance of 23.1% and a CP antenna bandwidth of 12.8%, along with a gain improvement of 1.5 dBi. The proposed antenna design was manufactured and tested, with the results closely aligning with the simulations, as shown within Figure 2.3.

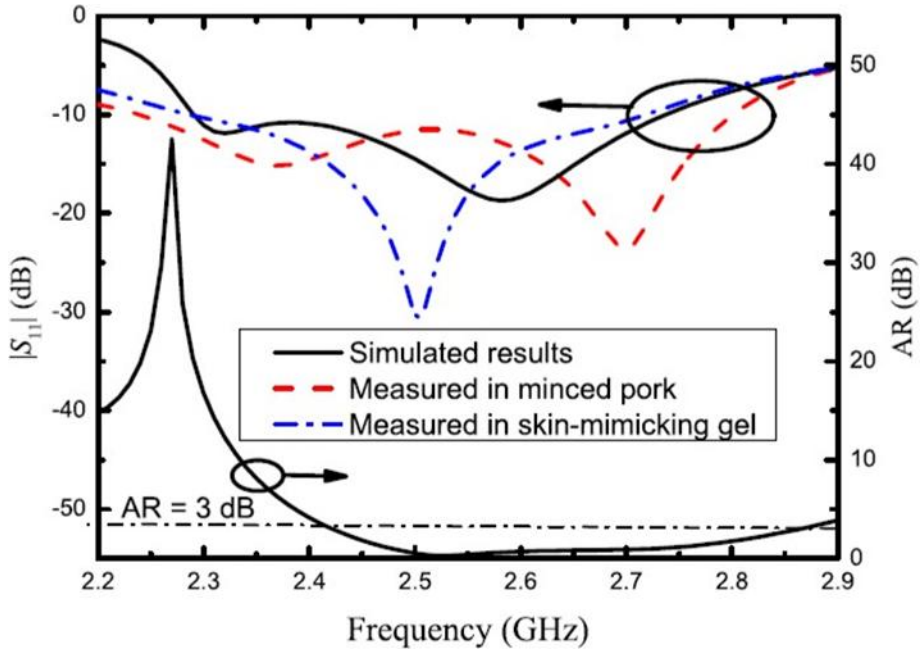

Figure 2.3: Circular polarization antenna measurements and simulations in various tissues (Xu, Jin, et al., 2020)

Additionally, the results of a previously developed sensor technique for gas spectroscopy alongside telemedicine assessment using human breath analysis are discussed by the authors in (Schmalz et al., 2017). A transmitter and receiver constructed with IHP's (0.13 µm SiGe BiCMOS) technology are integrated into the system. It makes use of a mm-wave/THz system with fractional integer-N phase-locked loops (PLLs) and convertible gas absorption cells with embedded antennas that function at 238–252 GHz and 494–500 GHz. The suggested sensor technique's construction is shown in Figure 2.4. The revised system achieves a time acquisition of 52 seconds as opposed to the prior 133 seconds and is more compact than the previous version.

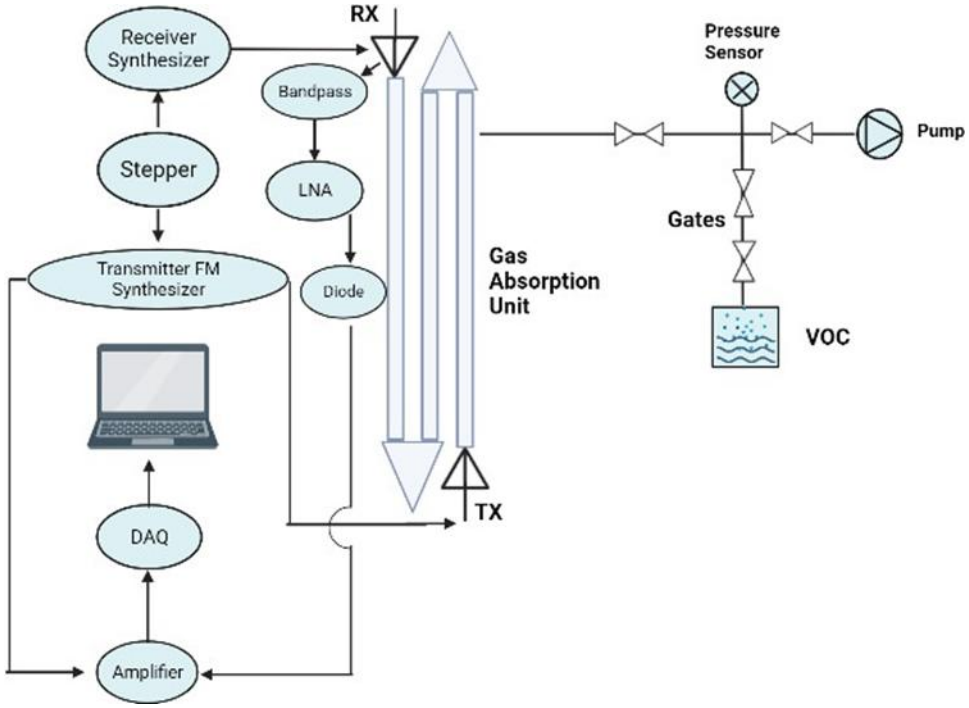

Figure 2.4: Absorption cell integrated with both transmitter and receiver gas spectroscopy sensors schematic (Dalloul et al., 2023)

Furthermore, an effective relative permittivity (ε_{eff}) three-layer model in human lossy tissue superstrate dual-band implantable antenna was described by (Xu et al., 2021). This antenna works in the ISM band as well as the 1.4 GHz wireless medical telemetry service (WMTS). Two arc-shaped tails with open ends were included in the antenna in order to accomplish circular polarization (CP). A CP 21.3% impedance bandwidth within the ISM band along with 10.38% bandwidth in the WMTS band was obtained by the experiment.

The authors of (Bharadwaj et al., 2017) describe a compact, cost- effective on-body antenna design that employs impulse wideband radio-ultra tech to detect 3D indoor limb body anatomy movements. Taking into account both LoS and NLoS routes, the body-centric wireless channel characteristics were analyzed, including parameters like Kurtosis, magnitude of path loss, multipath components, and the spread of RMS delay.

The implanted antenna's pulse-preserving ability was evaluated by analyzing received signal accuracy, which demonstrated 90% accuracy localization over 0.5-2.5 cm. Thus, this sensor design network significantly impacts patient monitoring and healthcare applications.

Additionally, the authors of (Sayem et al., 2019) examine the development of conformal wearable transparent antennas designed for wireless health monitoring and other real-time body-centric communication applications, especially for the elderly and dementia care. This design creates a simpler, affordable, robust, and flexible antenna by using a mesh conductive sheet using polydimethylsiloxane (PDMS) polymer as the substrate. To validate the design, a dual-band antenna prototype operates in the ISM and WLAN bands (2.33-2.53 GHz and 4.7-5.6 GHz). The gain and e□iciency were further enhanced using a two-layer conductor to improve RF performance.

Moreover, a human body-worn network design with twelve sensors is employed in (Bharadwaj et al., 2014) for indoor UWB human motion detection, which is useful for remote health monitoring. Different base stations, time of arrival (ToA), and first peak detection approaches are taken into consideration. To measure the absolute displacement error, a 2D localization error was obtained using 8 transmitters, and accuracy was assessed within the optical motion system. Comparing the resultant inaccuracy in commercial optical systems, it was one-third lower. Furthermore, the cuboid-shape configuration with 4 transmitters produced a 2-3% (accuracy reduction of 0.5–1 cm) average percentage error nevertheless the Y-shape configuration produced a 4% (accuracy reduction of 1-1.5 cm) error. The Y- shape is more straightforward and compact, which makes it appropriate for healthcare monitoring even with its marginally lower accuracy.

In (Peng et al., 2018), a WCE-based Impulse radio (IR) system for telehealth applications is utilized to investigate an on-body triband coil antenna. There are three frequencies at which the planned antenna can function. The paper first addresses a picture transmission technique using low-frequency multi-band communication. Furthermore, three wearable antennas with various parameters

were built and simulated to help the performance of the transmission. The findings demonstrated that, in comparison to the simulated values, 50 mm attenuation produced 32, 43, and 52 dB at the three operating frequencies, meaning 10.3, 13.3, and 16.4 dB more attenuation.

In addition, (Montaseri et al., 2023) a novel wearable antenna approach for wireless body area networks (WBANs) powered by the Internet of Medical Things (IoMT) is presented for use in health monitoring devices. The antenna network employs an elliptical leaky-wave antenna (LWA) positioned on the hubs in conjunction with Walsh-Hadamard coding to achieve simultaneous orthogonal signals and immunity from interruptions. The elliptical hub antenna and suggested sensors network are shown in Figure 2.5. The computed results were in agreement with the findings of the simulations and experiments, which showed better on and off-body connections than previous antenna designs. The two findings indicated 68° and 72° half-power beam widths in the Y-Z coordinates, respectively, and roughly radiation pattern ripples of 3 and 3.5 dBi in the X-Z plane.

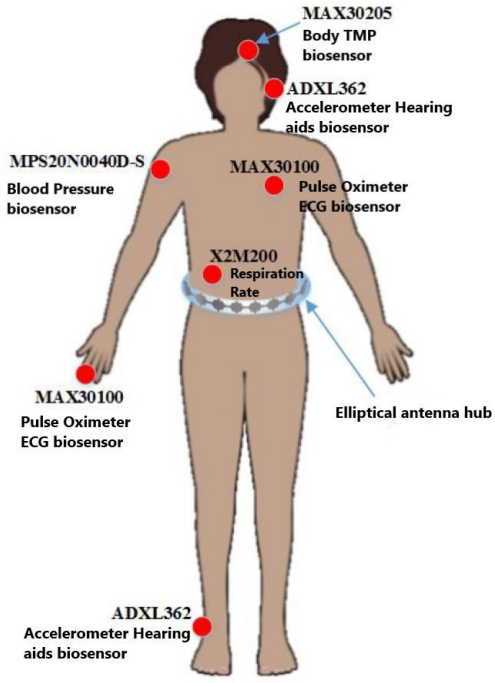

Figure 2.5: WBAN elliptical antenna system and sensors structure method based on IoMT (Montaseri et al., 2023)

Furthermore, (Omer et al., 2020) investigate the glucose sensitivity concentrations in low variation frequencies using a common coaxial probe kit in water-glucose tests, taking into account tangent loss and variations in the permittivity of the dielectric. The three concentrations data are presented in Figure 2.6. The Whispering Gallery Modes (WGMs) bio-sensor sensing system exploits the water-glucose relative permittivity in the 50–67 GHz mm-wave range, illustrated in Figure 2.7. Intending to provide continuous glucose monitoring for potential use in telehealth applications, this sensing structure tracks the magnitude and phase fluctuations of WGM. A (2.5–7.7 dB/[mg/ml]) sensitivity performance was demonstrated by the results.

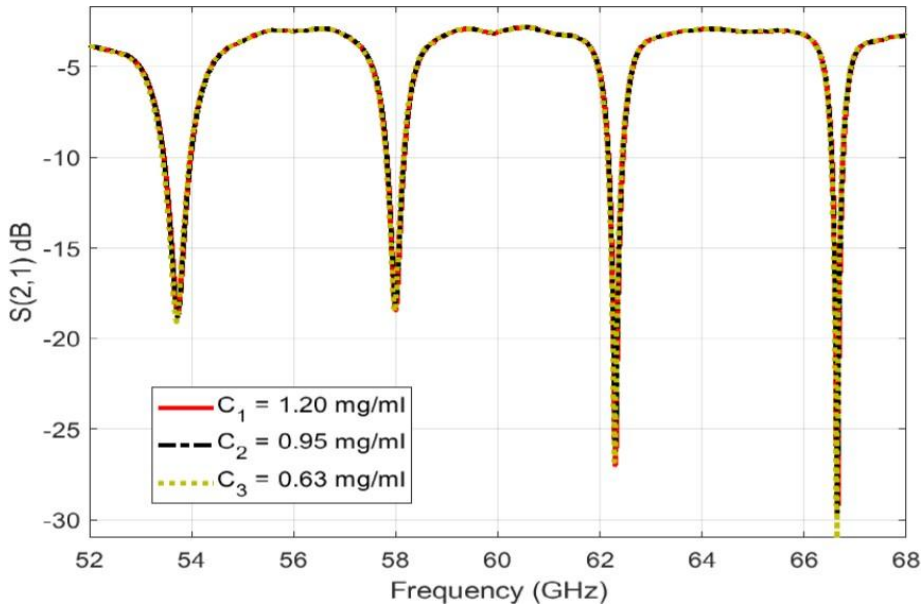

Figure 2.6: WGM resonance sensing measurements made at various glucose test doses (Omer et al., 2020)

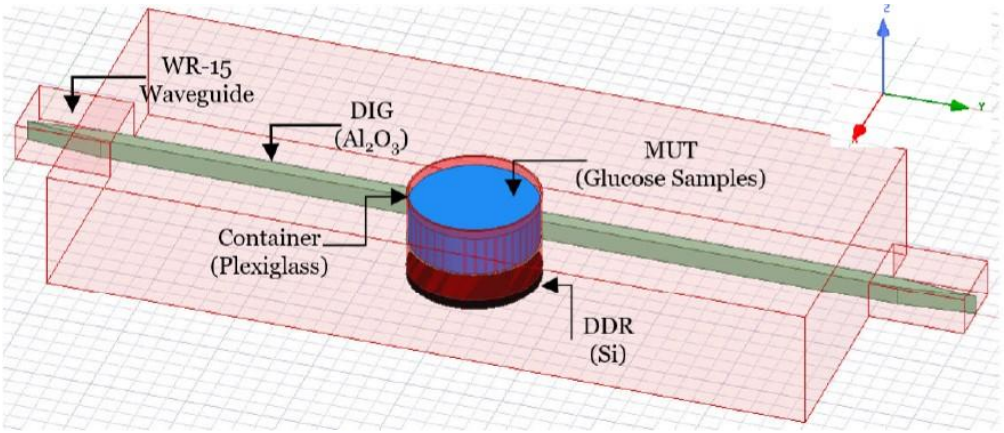

Figure 2.7: Wireless WGM sensor topology (Omer et al., 2020)

In (Rahmatinia & Fahimi, 2017), the authors present a hybrid approach that combines high-frequency excitation techniques with thermography for cancer detection purposes. This approach leverages both the temperature distribution and variation across the breast to predict the tumor's position and size. A direct association between temperature, specific absorption rate (SAR), size, and location is also shown via the heat transfer equation to identify the surface temperature distribution. Thus, potential applications for this design technique include remote patient monitoring with wearable technology.

In (Zerrad et al., 2023), a new UWB antenna design used in the detection of breast cancer is presented. Four star-shaped parasitic pieces, a rectangular slotted patch, and a tapering slot ground are all part of the design. Throughout its radiation bandwidth, the introduced antenna design obtains a 6 dBi realized gain as well as 80% e□iciency. Hence, it exhibits minimum signal distortion and provides great directionality. An antenna array was positioned above the breast to collect transmitted and reflected waves for cancer characterization in order to confirm the device's functionality and a breast phantom was made as well. The results of the detection of tumorous and benign breast tissue are shown in Figure 2.8.

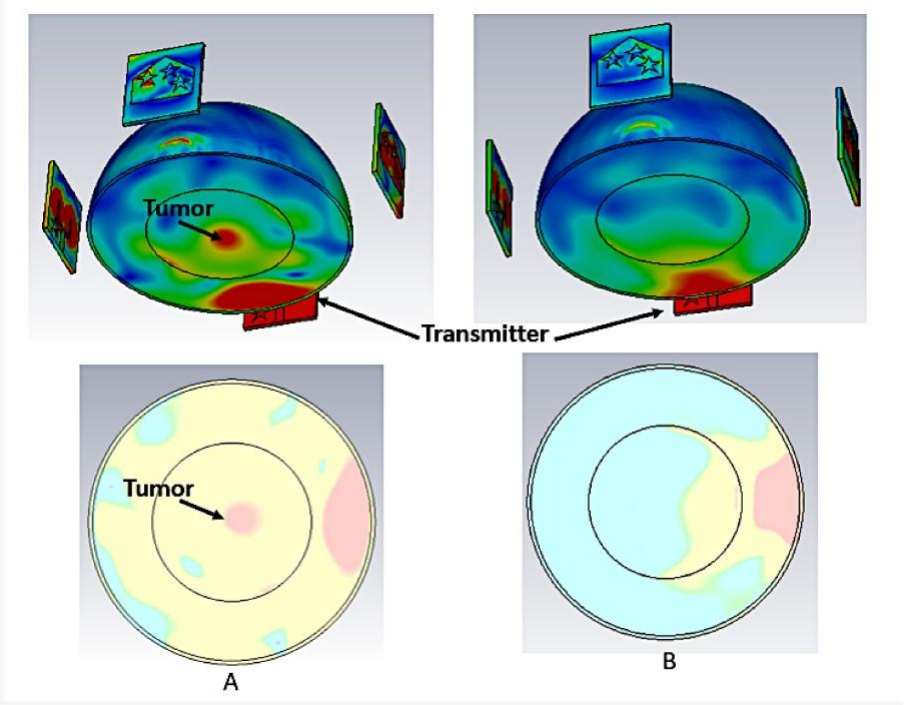

Figure 2.8: Tumor detection simulation results (Zerrad et al., 2023)

Moreover, a split-ring sensor resonator is employed in (Camli et al., 2017) to detect glucose and cancer. The frequency-dependent detection method is predicated on structural characteristics such as electrical permittivity. For glucose, glucose oxidase was integrated to give it biospecificity. Furthermore and following theoretical predictions, the 17.5 MHz frequency redshift in 15 minutes and 7.3% maximum error rate, together with 0.107 MHz/mgml^{-1} sensitivity validates the reaction to glucose DI water.

A metamaterial antenna array for visualizing and detecting breast cancers is presented in (Alibakhshikenari et al., 2020). Located around a breast model, the transceiver is made up of square concentric rings that are linked to a center patch. Concerning traditional patch antenna arrays, this topology obtains 11 dBi average radiation gain together with 18% e□iciency improvement. The antenna also shows a 30 dB average isolation among the radiators and S11≤ −20 dB average reflection coe□icient, which minimizes distortion and allows the detection of weak signals.

A radar system for remotely monitoring the human respiratory system is presented in (Sakamoto & Koda, 2020). The system employs continuous waves (CW) and is integrated with a two-dimensional nine-element antenna array design together with signal processing algorithms to function at 2.4 GHz. The measurements show that this design can successfully capture internal images of the respiratory system and accurately measure the breathing rate. Furthermore, the system's accuracy was validated by recording ribcage circumferences with a piezoelectric respiratory sensor. The final results indicate a 30 ms mistake in breathing interval estimation as well as a 0.05 m average imaging error.

Moreover, (Saeedkia et al., 2005) describe an imaging technique that investigates the usage of a photoconductive sensor and continuous-wave terahertz array, emphasizing the terahertz rays' characteristics. By employing an array operating at 1 THz, this system achieves lower μW terahertz power levels while simultaneously improving terahertz power output and consuming less power. Additionally, the analysis focused on how the applied DC bias and beat frequency affected the radiated power. The radiation path could be guided by more than 30° via varying the angle among the two laser rays, hence qualifies the method for medical imaging and monitoring applications.

The work in (SalmanOgli & Rostami, 2013) explores the connection within dye molecule fluorescence with surface plasmon resonance (SPR). The primary goal is to optimize nearfield amplification by making use of plasmon hybridization modes within nanoparticles. This is important because it will extend the lifespan as well as enhance dye quantum e□iciency within deep-tissue scanning for telemedicine uses. Also, it investigates the use of strong plasmon resonance nanoparticles (NPs) to broaden the visible near-infrared (NIR) spectrum. Variables like the radius and surface distance of the NP, as well as the thickness of the inner and outer shell layers, were associated with an increase in fluorescence.

A wireless, batteryless trimodal brain interaction system-on-chip (SoC) is presented in (Jia et al., 2020). The SoC has two sets of sixteen channels each for brain recording and optical stimulation, in addition to eight channels for

electrical stimulation. Four paralyzed rats were used for in vivo and in vitro, testing of the system, and the outcomes demonstrated that the trimodal SoC successfully caught neurons and tissue reactions. This indicates that a wide range of wireless patient monitoring applications could benefit from it.

2.2 CURRENT METHODS AND APPROACHES IN REMOTE HEALTH MONITORING

Two essential variables in systems that monitor health remotely are the type of devices used and the techniques employed. A comprehensive overview of the several health monitoring equipment was given in the preceding section. This section will focus on the different methods implemented in these systems. Some studies have explored channel characteristics for the aforementioned devices, while others focus on advancements in wireless capsule endoscopy (WCE). There is also work on sensing and imaging techniques.

Impulse response analysis is applied in (Hwang et al., 2015) to examine a channel approach to human body communication (HBC). The study analyzes impulse response magnitude and phase as random variables evaluated on 70 human participants using the optical-synchronization approach, in order to mimic channel fluctuations over a broad frequency range (5-80 MHz). Additionally, the signal loss varies for each HBC user due to differences in dielectric properties. Tests for evaluating the random variables' normality revealed that they had a uniform distribution with an identifiable mean and standard deviation. Moreover, the outcomes showed dependence between the impulse responses at the sampling point, indicating the model's suitability for credible data transfer in medical applications.

Furthermore, data rates, resolution, and power of transmission among both in and on-body ultra-wideband (UWB) channels of communication are investigated by (Floor et al., 2019), with a focus on the initial disease detection in telemedicine using WCE. In three different scenarios, the power was assessed utilizing quadrature phase shift keying (QPSK) modulation, channel capacity,

and a combination of PPM and QPSK modulation using Reed-Solomon (RS) coding for the channel. The results show that power e□iciencies occur at lower frequencies, and that capacity and transmitted power do not change even at higher bandwidths than 1 GHz. Furthermore, PPM and QPSK's performance differed very little.

In addition, (Mollah et al., 2021) present a bio-sensor channel of dual-analyte that combines surface plasmon resonance (SPR) with a very sensitive photonic crystal fiber (PCF) construction. Also, using the finite element method (FEM), the sensor architecture was characterized and shown to have 2,792.97 RIU^{-1} amplitude sensitivity (AS) as well as 186,000 nm/RIU wavelength sensitivity (WS). This bio-sensor shows promise for health monitoring applications, particularly in detecting biomolecules and other biological analytes.

Moreover, interbody channel characteristics for in vivo wireless sensor systems using nanotechnology are investigated by (Elayan et al., 2017) at both optical frequencies (400–750 THz) along with terahertz bands (0.1–10 THz). This work has implications for precise diagnosis of illnesses and intrabody health tracking, among other fields. The computation of path loss took into account both small and large-scale scattering, waves propagating impact, and the absorption of molecules in human tissue. Model validation was accomplished by means of Electromagnetic simulations, which confirmed analytical results. The paper also discusses the link budget for nanodevices in the human body, emphasizing receiver sensitivity, path loss, and transmission power for photonic and terahertz equipment.

Furthermore, a body antenna network (BAN) intended for power-su□icient wearable medical sensors and wave propagation close to the body's skin is investigated in (Lea et al., 2009). The system operates with band-aid antennas with the help of the Norton wave process. The thinner outer layers of the body surface were found to be insignificant at a frequency of 3 GHz, and a two-layer structural model was determined to be su□icient to compute path gain. Short-range path gain is frequency-dependent; however, employing ultra-

wideband (UWB) leaves the Norton surface channel dispersion less, which is advantageous for communication. Also, the suggested design is contrasted in the study with other published experiments.

In (Maity et al., 2019), the authors present an evaluation of the performance of a multi-data rate receiver that allows frequency-modulated (FM), amplitude-modulated (AM), and continuous-wave (CW) broadband human-body communication. WBAN-based health tracking applications benefit from enhanced safety and energy conservation due to this technique. The receiver obtains a signal-to-interference ratio (SIR) of 22 dB e□iciency across AM and FM techniques, according to the simulation results that are presented. Additionally, an oscilloscope designed to detect signals from the human body reveals a 10^{-4} bit error rate (BER) for all FM, AM, and CW methods, with a -21 dB e□iciency in interference rejections.

A backscatter radio frequency system intended for remote excessive data-rate communication with deep medical devices in (Khaleghi et al., 2019) is presented. Furthermore, Considering the removal of the transmitter at the implant, this approach reduces power usage by 20–45 mW and allows for remote data processing. For wireless capsule endoscopy (WCE), the system employs the use of a self-resonant configurable antenna that produces a significant cross-section of radar. In order to strengthen the backscatter connection and the implant's ability to read information, a bistatic wearable antenna design is suggested. The design was tested on liquid phantoms and in vivo animals, and it was confirmed using numerical simulations. According to the results, the capsule used a 250 mW reader power to obtain scatters back data rates of 1 and 5 Mb/s at 13 cm depth.

Moreover, the work of (Khan et al., 2018) investigates the GI tract navigation and wireless capsule endoscopy (WCE) positioning device for monitoring patients from afar. The position of the capsule within the stomach, small intestine, and large intestine was ascertained using a 3D full-wave human tissue simulation. The research studied crucial aspects influencing location reliability, such as the arrangement of the sensor array, tissue features, and the

number of capsules. It also considered cases where the transmitted signal followed a specific probability distribution. Results from the computational solver showed that the number of external antenna receivers significantly influenced localization accuracy, more so than the number of capsules used. Moreover, the power distribution had the greatest impact on the large intestine.

The authors of (Shoaib et al., 2019) examine a variety of methods for improving optical brain imaging (OBI) systems' spatial resolution. OBI devices have limitations in terms of spatial resolution, especially for brain imaging, even though they are more affordable, portable, and user-friendly than other medical imaging methods. Two major limitations include the low penetration of near-infrared (NIR) light through deep tissue and the unpredictable path of NIR photons. Also, it discusses the OBI systems concepts and boosting spatial resolution issues. Additionally, it provides an overview of different approaches to resolving these problems and compares them with other imaging systems that have higher spatial resolution. One such technique for improving spatial resolution involves assessing two different brain regions, as shown in Figure 2.9.

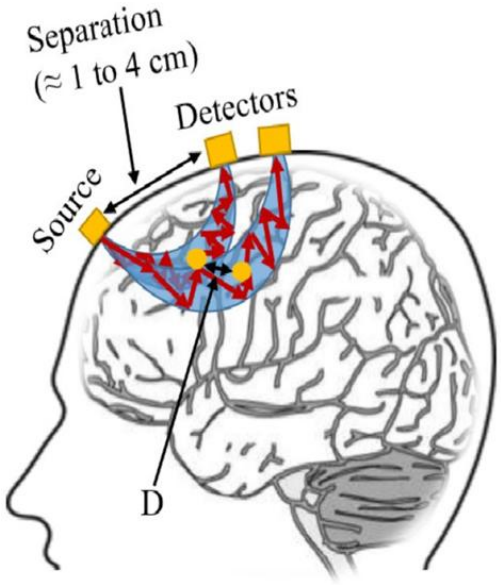

Figure 2.9: A demonstration of the technique for improving optical brain imaging by locating specific brain regions over a given distance (Shoaib et al., 2019)

Moreover, (L.-Y. Ma & Soin, 2022) provide physical detecting devices overview including their materials, performance, printing methods, and interface circuits for worn monitoring of health purposes. These sensor devices are intended to track biometric variables like mobility strain, skin temperature, and pulse wave pressure. The article also examines the architectures and functionalities of printable interface design coupled with sensors on clothing, highlighting current developments in this field. Also, Thin-film transistors, digital circuits, antennae, and amplifiers, together with interconnects are interface circuits with different examples.

The distortion of transmission information resulting from surface wave propagation and complicated electromagnetic (EM) wave diffraction is studied in (Koutsoupidou et al., 2020). The study utilizes two antennas to assess transmission variations in a millimeter-wave glucose sensing system. Numerical simulations combined with glucose-related experiments showed that undesired multipath transmissions had a substantial effect on the signals received. Nevertheless, the use of absorbers surrounding the skin prototype with the sensor-equipped antennas helped to address the problem. As a result, transmission modifications (ΔS_{21}) show that the suggested glucose sensing system's sensitivity was increased.

Furthermore, (Fawole & Tabib-Azar, 2016) investigate near-field THz imaging to address the challenges of spatial resolution in imaging applications using various biological samples. The design combines a horn antenna with Teflon, quartz, and metal probes for imaging applications. These probes were used to image the wing of an insect, the brain of a mouse, and a leaflet of a dwarf umbrella tree. The mouse brain's imaging results showed different areas within specific parts, however the leaflet's venation was clearly apparent. Furthermore, compared to optical imaging, the bug wing imaging showed a corium shift towards membrane areas exhibiting a distinct profile. For additional imaging applications, a dielectric slab comprising an interior framework was used in another solution.

In addition, (Zhao et al., 2022) present an imaging system consisting of a thermoacoustic ultrashort pulse microwave to ease the limits in large-field imaging. The design has a 14 cm × 14 cm imaging view, 7 cm imaging depth, microwave radiation of 40 cm × 27 cm, and 290 μm resolution. Furthermore, design performance was evaluated using an in vivo cancerous tumor of a human breast implanted inside an ewe breast phantom (π × 5 cm × 5 cm) with a tumor-to-background contrast ratio of 1:2, as well as breast tumor phantoms of various forms. The results demonstrated the system's capability to accurately detect breast tumors, indicating its potential use in breast screening applications.

CHAPTER 3

3. MACHINE LEARNING CHANNEL PARAMETER ESTIMATION IN VLC-BASED MEDICAL BODY SENSOR NETWORKS

3.1 OVERVIEW OF MACHINE LEARNING CHANNEL PARAMETER ESTIMATION IN VLC-BASED MBSNS

A significant advancement in wireless connectivity is brought about by the Sixth Generation (6G) communications evolution, which enhances the capabilities of networks with Ultra Reliable Low Latency Communications (URLLC), Enhanced Mobile Broadband (eMBB), Massive Machine Type Communications (mMTC), and huge information communications. This creates opportunities for novel services and applications, as illustrated in Figure 3.1. Table 3.1 shows the main service contrasts between Fifth Generation (5G) and 6G utilizing a variety of key performance indicators (KPIs). Furthermore, 6G makes use of machine learning (ML) and artificial intelligence (AI) (P. Mitra et al., 2021; Yang et al., 2019) to facilitate context-aware communication, improve security, dynamically allocate spectrum, and maximize network administration. 6G is a revolutionary development in wireless technology given the incorporation of ML, which guarantees clever, flexible structures that support self-governing systems, distribute resources effectively, and provide individualized communication experiences (Kaur & Khan, 2022; Kaur et al., 2021). In order to emphasize the advantages of applying ML within wireless communication systems, the work in (Xiao et al., 2022) introduced a deep learning (DL) framework designed for modeling link-level Multiple-Input Multiple-Output (MIMO) channel conditions.

They validated the proposed model using cross-validation methods and power analysis, confirming its efficiency, reliability, and consistency in performing DL-based Channel State Information (CSI) feedback tasks.

In addition, a promising integration to the 6G is Visible Light Communication (VLC) technology which maximizes regular indoor applications like transmission of data and indoor positioning by offering the potential to exchange information within the spectrum of visible light.

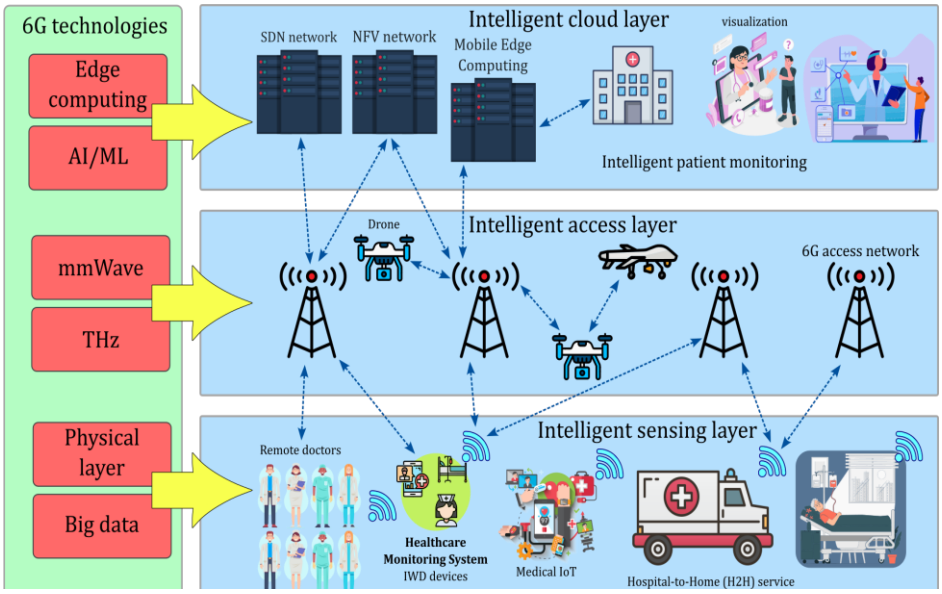

Figure 3.1: The architecture vision of 6G (Antaki et al., 2025)

Furthermore, incorporating VLC into 6G systems overcomes connectivity. Challenges through offering hybrid communication networks that leverage the combination of VLC and radio frequency to address network issues in densely populated areas or high interference from electromagnetic wave areas. For critical 6G services such as the Internet of Things (IoT) and healthcare settings, these hybrid systems use VLC capabilities to improve security in line-of-sight contexts (Ariyanti & Suryanegara, 2020) while offering higher data speeds and reliability.

Additionally, the introduction of VLC-based Medical Body Sensor Networks (MBSNs) through 6G networks has been a remarkable development in the healthcare sector since it would facilitate efficient communication among external equipment and medical sensors. In healthcare settings like clinics and hospital facilities, there is a growing need for a variety of technologies, including the Internet of Medical Things (IoMT), Wireless Sensor Networks (WSNs), Biomedical Signal Processing, and Telemedicine. These technologies employ real-time biological variable tracking to provide prompt interventions and early identification of health hazards. To showcase the potential of ML in WSNs, the study in (Fei Chengweiand Liu, 2021) underscores the increasing significance of ML in advancing Wearable Health Monitoring (WHM) systems. It contrasts traditional ML methods with newer DL techniques like Sparse Coding autoencoders and Recurrent Neural Networks (RNNs), highlighting their superior performance in handling time-series sensor data, enabling automated feature extraction, recognizing user activities, and achieving more accurate classifications. Building on this, the research in (Manikandan et al., 2025) introduces a DL-based WSN architecture aimed at real-time health monitoring and disease diagnosis. Their approach achieved a 96% classification accuracy and a low error rate of 0.08, outperforming conventional models by over 5% in accuracy, thereby reinforcing the value of ML integration in VLC-enabled WSNs for enhanced healthcare reliability and performance. Furthermore, embedding a VLC-based MBSNs into the 6G infrastructure proves pivotal for applications like electronic health (eHealth), indoor localization, underwater data exchange, and advanced sensing systems. As demonstrated in (Niarchou et al., 2021), VLC-powered MBSNs facilitate high-precision tracking and sensing, key components in supporting massive IoT deployments and URLLC requirements of 6G. Moreover, the incorporation of AI and ML into these networks addresses critical challenges, such as Light Emitting Diode (LED)-induced nonlinear distortions, variable environmental conditions, and system security flaws. This integration enhances essential tasks like phase and channel estimation, modulation detection, and real-time positioning (V. N. Saxena et al., 2023).

Ultimately, this synergy contributes to robust, high-capacity, and dependable communication systems aligned with 6G's objectives for smarter resource management, enhanced security, and intelligent connectivity.

Table 3.1: 5G and 6G communications KPIs comparison (Antaki et al., 2025)

KPI	5G	6G
Traffic Capacity	10 $Mb/s/m^2$	~1-10 Gb/s/m3
Data rate: downlink	20 Gb/s	1 Tb/s
Data rate: uplink	10 Gb/s	1 Tb/s
Uniform user experience	50 mb/s, 2D	10 Gb/s, 3D
Latency (radio interference)	1 ms	0.1 ms
Jitter	Not Specified	1 µs
Reliability (frame error rate)	$1\text{-}10^{-6}$	$1\text{-}10^{-9}$
Energy/bit	Not Specified	1 pJ/b
Localization precision	10 cm in 2D	1 cm in 3D

Designing various medical facility scenarios, including intensive care units (ICU), semi-private patient rooms, family-type patient rooms (FTPR), and clinics, requires diverse key criteria. Important concerns like latency, electromagnetic interference (EMI), security, and health hazards related to exposure to radio frequency (RF) technology are all addressed by VLC-based MBSN networks in healthcare settings. Among several advantages of VLC which provides immunity to interference of RF, non-interference with medical equipment, and improved security by preventing eavesdropping. The authors in (Zwaag et al., 2021) used an ICU environment to test a Manchester On-Off-Keying (OOK)-based VLC system in order to demonstrate the usefulness of VLC in healthcare environments. In addition to successfully monitoring critical indicators like the heart rate, saturation of oxygen, and blood pressure, this system achieved Eye Opening Penalty (EOP) values of 0.89, 0.96, and 2.67 dB over transmission distances of 1.5 m, 5 m, and 15 m, respectively. This helped to stop the spread of disease. Also, utilizing WSNs positioned on essential

biological areas such as the shoulder, wrist, or ankle allows MBSNs to gather unique information from the worn sensors within patients' bodies in order to collect maximize vital signs, reduce interference, ensure ease of use, and offer biomechanical stabilization. In applications such as the exchange of real-time health information, embedded medical device advancement, remote and continuous surveillance of patients, and personalized healthcare, leveraging VLC can assist in promoting security, efficiency, and reliability of medical data interchange within healthcare technology. Thus, delivering improved diagnosis, care, and overall health results is a significant step toward creative and patient-centered healthcare solutions.

To tackle the real-world challenges of deploying MBSNs systems in hospital environments, the study in (Guaña-Moya et al., 2024) presents a thorough survey of VLC-based eHealth solutions, with a particular emphasis on modulation schemes and channel coding strategies. The paper not only reviews various research efforts, including hands-on implementations, but also points out key obstacles that remain, such as the need for more efficient channel coding methods and the development of hybrid VLC-RF systems to ensure stable performance in dynamic and non-line-of-sight hospital settings. In a related effort,(Celik et al., 2022) offers an in-depth analysis of Internet of Bodies (IoB) technologies, addressing the complexities involved in modeling due to the human body’s diverse dielectric properties. It highlights electro-quasistatic human body communication as a strong candidate, offering advantages like minimal signal leakage and enhanced data security. The paper also stresses the importance of improving channel estimation techniques and enforcing stricter privacy measures. Likewise, the study in(Celik & Eltawil, 2022) examines communication methods within IoB systems, comparing conventional RF-based approaches with body-coupled communication, which stands out for its higher data rates and energy-saving potential. Although both surveys include experimental results, they point to several persistent issues, such as the lack of accurate modeling tools, signal interference in multi-user scenarios, and the absence of unified communication standards.

These limitations underline the ongoing need for deeper research and stronger regulatory frameworks to build secure, efficient, and interoperable MBSN solutions for healthcare applications.

Integrating IoT into healthcare systems offers significant advantages, including continuous monitoring and better overall patient care. However, it also raises important ethical concerns. One major issue is informed consent, as the ongoing and often passive nature of data collection in IoT setups can leave patients unaware of the full extent of what is being monitored. Protecting sensitive health data from unauthorized access is another major challenge, alongside the need to maintain data integrity to avoid errors in diagnosis or treatment. Privacy risks also emerge due to the potential for data interception during wireless transmission. Ensuring proper access control is vital to prevent exploitation or misuse of personal medical data. To address these challenges, the study in(Zakerabasali & Ayyoubzadeh, 2022) emphasizes the use of encryption techniques, secure cloud infrastructure, and strict access control systems. Expanding on this, the authors in(Subramaniam et al., 2023) proposed a privacy-preserving and interoperable IoMT framework tailored for remote healthcare use. Their system includes features like device authentication, low-power clustering, environmental sensing, data verification, and secure encryption, all aimed at boosting network reliability and safeguarding patient information. Their method showed strong results, with a 20% boost in data rate, a 15% drop in packet loss, a 35% extension in network lifetime, and a 10% decrease in both energy use and communication delays. Additionally, VLC-based MBSNs can play a key role in strengthening ethical standards by taking advantage of their secure transmission capabilities to protect patient data and uphold privacy in healthcare environments.

Furthermore, a variety of VLC channel parameters, including Root Mean Square (RMS) delay spread and DC channel gain, are crucial for accurately regulating the system's entire efficiency. According to (Zhu et al., 2022), current developments in modeling of VLC, like the proposed 3D space-time-frequency geometry based stochastic model (GBSM), have shown capabilities

in capturing distinctive indoor VLC channel characteristics, such as non-stationarities and light-emitting diode (LED) radiation patterns and receiver influence movements. DC channel gain parameter represents attenuations of the transmitted signal that influence the strength of the received signal and, consequently, affect the signal-to-noise ratio (SNR). A higher DC channel gain can help lower path loss, but it also causes the signal to weaken more over long distances. This means the system's performance can suffer because the signal received at the other end isn't as strong. Likewise, the RMS spread, which represents the temporal dispersion of the received signal, describes the propagation impact of the multipath across the communication channel. The multipath effects, in which transmitted signal delayed duplicates interact with the original signal, resulting in intersymbol interference (ISI) and thus lowering quality of communication, are directly shown by this temporal dispersion. This measure helps design equalization approaches to reduce ISI and gives an understanding of channel behavior within VLC-based MBSNs, allowing for higher data rates and secure transmission in dynamic situations. The efficiency and dependability of VLC systems can be improved by comprehending and reducing both factors.

Several approaches are used in VLC to create reliable and effective communication networks; however, in order to overcome such challenges, it is essential to make accurate estimates of the key channel characteristics in the VLC environment. For this reason, VLC offers a variety of useful strategies. Among these is the channel-sounding approach, which uses pilot signals or training sequences to express the receiver's channel response. Furthermore, the channel's response, that is expressed by recognized impulses and provided as pilot signals or training sequences, can be examined using the channel impulse response (CIR) technique. Also, frequency-domain, time-domain, statistical modeling with Rayleigh or Rician distributions, and other techniques are frequently used to estimate significant parameters like propagation of multipath components, delay spread, and the ratio of SNR. Moreover, there are impressive possibilities for channel characteristics estimation within VLC systems once ML

is integrated in order to learn complex patterning and determine channel parameters from transmitted and received data. These cutting-edge techniques show potential in accurately calculating channel characteristics within VLC systems, which will improve efficiency as well as reliability. A data-driven method for handling challenging communication settings is provided by using ML-based channel estimate processes, which ultimately results in more resilient and adaptable VLC systems.

3.1.1 Ml Approaches For Channel Parameter Estimation

In order to improve the effectiveness and resilience of state-of-the-art technologies like VLC networks, ML approaches must be employed. This will help to solve practical issues like nonlinear distortion, security, jitter, localization accuracy, and estimation of channels. ML efficiently reduces fading effect, increases rate of convergence, and strengthens the network's protection against eavesdropping by utilizing a different approaches. Additionally, such techniques analyze enormous data to identify correlations across variables that affect signal propagation, reducing illumination noise, scattering, and signal distortion. Thus, in VLC implementations these models allow for the construction of systems with high location accuracy, decreased errors, and enhanced performance (V. N. Saxena et al., 2023).

Despite such difficulties, precise prediction of the channel parameters is significant since it has a direct impact on the ability of the system for modeling transmission settings, maximize efficiency, and sustain reliable communication in a variety of scenarios. As a result, we examine a number of crucial ML techniques in this subsection that have shown promise in estimation of channel parameter for wireless setting. Among these methods are elementary, widely used methods including Linear Regression (LR); more sophisticated models like K-Nearest Neighbors (KNN) together with Support Vector Regression (SVR); and sophisticated RNN structures with their variations, such as vanilla RNN, Gated Recurrent Unit (GRU), and Long Short-Term Memory

(LSTM). Every approach has different benefits, from simple interpretability to complex modeling of sequential dependencies.

In order to provide an initial description of the relationship between the input of independent variables and the output of dependent variables, a statistical supervised linear regression (LR) ML method is utilized. This initial data investigation is then useful to assist in choosing more complex ML methods since it is perfect for studying trends and forecasting outcomes due to the linear relationship assumption between the variables (Maulud & Abdulazeez, 2020).

Moreover, another supervised non-parametric ML method used for classification and information estimation is K-Nearest Neighbors (KNN). The fundamental idea behind KNN is to classify or predict outcomes based on the degree of similarity between the input elements. This is accomplished by employing distance metrics such as the Euclidean, Manhattan, Minkowski, and Hamming distances to compare data points inside the feature space (Rahman et al., 2024). For continuous regression tasks, the output is calculated by averaging k-nearest neighbors' values, but for discrete classification cases, the majority within these neighbors is used to decide the result (Zhang, 2022).

Additionally, Support Vector Machines (SVM) can be extended to estimate nonlinear and linear data using Support Vector Regression (SVR) which is considered a supervised model (Zhou et al., 2021). By establishing an epsilon-tube margin that excludes true output deviations, SVR reduces estimation error while concentrating on minimizing outside margin errors. This method focuses on necessary errors instead of improving the whole dataset, which helps SVR process information with greater efficiency. SVR finds the best hyperplanes for precise predictions by mapping input parameters onto higher-dimensional spaces (Yu et al., 2022).

Moreover, applications involving data sequence estimation, including large modeling of languages, text generation, recognition of speech, forecasting time series, and the analysis of videos, frequently employ Recurrent Neural Networks (RNNs) which is a class of deep neural networks. RNNs' memory component allows the usage of data from prior sequences to generate new

results (Gizzini & Chafii, 2024). The vanilla RNN represents the simplest form of this architecture and works well for short estimation sequences in which generating is dependent on the latest inputs only (Mao & Sejdić, 2023). whereas working with long sequences of data have difficulties detecting long-term dependencies since they only store data from the recent few outputs. This limitation, known as the vanishing gradient problem, stops the network from efficiently obtaining long-sequence data.

Furthermore, the Gated Recurrent Unit (GRU) is a powerful RNN variation with a simpler gate topology (Zengeya & Vincent Fonou-Dombeu, 2024). An update gate (z_t) and a reset gate (r_t) make up the GRU's gate structure, which preserves both efficiency and performance. Due to their different responsibilities for determining how much of the prior output should be disregarded or used in the subsequent stage, both gates determine the flow of the data through ML (Brandão Lent et al., 2022).

3.1.2 Related Works

To examine ML-based channel estimation in VLC infrastructure, (Játiva et al., 2021) investigate an Extreme Learning Machine (ELM) for equalization and channel prediction in VLC systems utilized in underground mining settings. In order to enhance bit error rate (BER) performance, the suggested ELM-based system makes use of single-layer feedforward networks (SLFN). Moreover, leveraging artificial neural network (ANN) based ML, the authors in (Alkandari et al., 2023) investigate visible light positioning (VLP) error performance which uses both indoor system positioning and VLC for 3D indoor drone localization. Significant improvements in drone localization accuracy are shown by the outcomes.

In a similar manner, by using an XGBoost position estimator, (Du et al., 2021) present an ML-based VLP system for quicker deployment than ML-regression approaches within Industrial Internet-of-Things (IIoT) applications. Furthermore, to improve the indoor estimation of channels in VLC systems, the work in (Razaz et al., 2024) makes use of LSTM. The findings show that the

LSTM-based predictor performs better than the conventional Kalman filter (KF) estimator, offering enhanced BER and better channel estimation.

Further LSTM channel estimation in a non-linear VLC system using optical Intelligent Reflecting Surfaces (IRS) is shown in (Sharma et al., 2023). According to simulation results, the LSTM approach performs better than conventional channel estimate algorithms in terms of detection of signals and reliability, highlighting its great potential for reducing distortions and preserving efficient communication in realistic VLC conditions. Moreover and in (Z. Ma et al., 2022), the researchers present a performance comparison of the channel estimation among three ML methods in a multi-wavelength VLC network. In comparison to other methods, the study demonstrated the fact that the Sparse Autoencoders (SAEs) algorithm offers the best channel estimation performance.

Additionally, in a vehicle-based V-VLC scenario, (Ullah et al., 2023) employed a hybrid Deep Neural Network (DNN) that consists of a multilayer perceptron (MLP), bidirectional LSTM, and GRU for path loss estimation and jamming detection. In comparison to existing models, examinations showed satisfactory results for the purposes of accuracy and minimizing error. Additional research in (Salama et al., 2023) compared DNN, YOLO v3, and Kalman Filter algorithms with three distinct modulation schemes to improve channel estimation by decreasing BER in indoor VLC systems. The findings indicate that. DNN outperforms KF, and YOLO v3 optimization improves channel estimation more effectively than traditional techniques.

The authors of (R. Mitra & Kaddoum, 2022) present a novel ML technique based on Random Fourier Features (RFF) in a nonlinear VLC channel. Findings indicate that RFF performs better in situations involving limited data, with a lower training approximation and higher classification accuracy. Furthermore, (Naser et al., 2022)describe the use of Federated Learning (FL) in VLC systems to tackle challenges such as privacy issues and performance of communication in conventional centralized ML techniques, highlighting important design elements meant to increase system resilience and effectiveness. An overview of all current ML-based VLC channel prediction methods is shown in Table 3.2.

Table 3.2: ML-based VLC channel estimation studies (Antaki et al., 2025)

Papers	Method	System Model	Machine Learning improvements
(Játiva et al., 2021)	Extreme Learning Machine (ELM)	VLC Underground mining system	Better BER in challenging circumstances exceeds conventional techniques and produces performance almost ideal in channel estimation.
(Alkandari et al., 2023)	Artificial Neural Network (ANN)	3D VLP Industry channel conditions system.	Higher accuracy and lower positioning errors in the smoke channel.
(Du et al., 2021)	XGBoost ML	Smart Trolley's Indoor VLP positioning system	Reduced training time, and maintained positioning accuracy to improve deployment speed.
(Razaz et al., 2024)	Long Short Term Memory (LSTM)	Indoor VLC channel	Lower BER which achieves better accuracy and system robustness.
(Sharma et al., 2023)	Long Short Term Memory (LSTM)	Non-linear VLC IRS-aided system	LSTM performance is better than traditional approaches.
(Z. Ma et al., 2022)	LSTM, GRU, and SparseAutoencoders (SAEs)	VLC Multi-wavelength system	SAEs have higher channel modeling performance.
(Ullah et al., 2023)	Hybrid DNN	Vehicular (V-VLC) and IEEE 802.11p network systems	Reduced estimation error and high detection accuracy.
(Salama et al., 2023)	DNN, YOLO v3, and Kalman Filter	Indoor different modulation VLC system	Among modulation techniques, DNN minimizes BER lower than KF.
(R. Mitra &Kaddoum, 2022)	Random Fourier Features (RFF)	Nonlinear VLC systems	Enhanced accuracy with reduced training complexity.
(Naser et al., 2022)	Federated Learning (FL)	Various VLC network applications	Higher performance and privacy with lower transfer data cost.

3.1.3 Contributions

The work focus of this chapter within this dissertation is succinctly described below:

• In order to characterize channels, we use an advanced ray tracing approach (Donmez et al., 2021). By integrating parameters of the user random mobility model and artificial structures onto the channel model while adhering

to illumination requirements, we are able to construct CIRs that are customized to a realistic hospital environment. Our method takes into account physical aspects including diffuse and specular reflections, characteristics of wavelength-dependent reflection, real light sources, and up to 10 reflection orders.

• In order to improve reliability and enable resilient 6G health monitoring application networks, we developed ML-based reliable methods for assessing path loss and RMS delay spread in VLC-based MBSNs.

3.2 SYSTEM MODEL

3.2.1 Mobile Channel Model For Vlc-Based Mbsns

Many techniques are used to precisely predict the characteristics of VLC channels, with Zemax® (SMART Research Program L113955) ray tracing software being a popular method. The sequential ray tracing approach in the software is perfect for imaging applications where it tracks rays between both transmitter and receiver over a series of surfaces, hitting each other once. However, rays may reflect and disperse in any order around the setting using non-sequential ray tracing method. Therfore provides higher realistic propagation scenarios that take into consideration intricate interactions with furniture, medical devices, and human bodies. The non-sequential method offers a more thorough CIR estimation by precisely capturing such relationships, which increases accuracy and dependability (Gu et al., 2024).

Therefore, we apply the methodology of site-specific non-sequential ray tracing that is presented in Figure 3.2 and further explained in (Donmez & Miramirkhani, 2021). CAD objects are first arranged to create 3D realistic hospital settings utilizing real-life data, as shown in Figure 3.3. Furthermore, wavelength dependence is taken into consideration while specifying CAD object reflectance surfaces. After that, the configuration of the photodetectors (PDs) and luminaires is arranged, and their specifications are established effectively. Depending on the position of the body within each sample point

along a trajectory, the sensor nodes' parameters of orientation are connected to detectors on the shoulder, wrist, and ankle are placed, respectively. In order to generate several sample points over different paths in each scenario, a random trajectory generator is used, taking into account starting points, directions, and random step lengths.

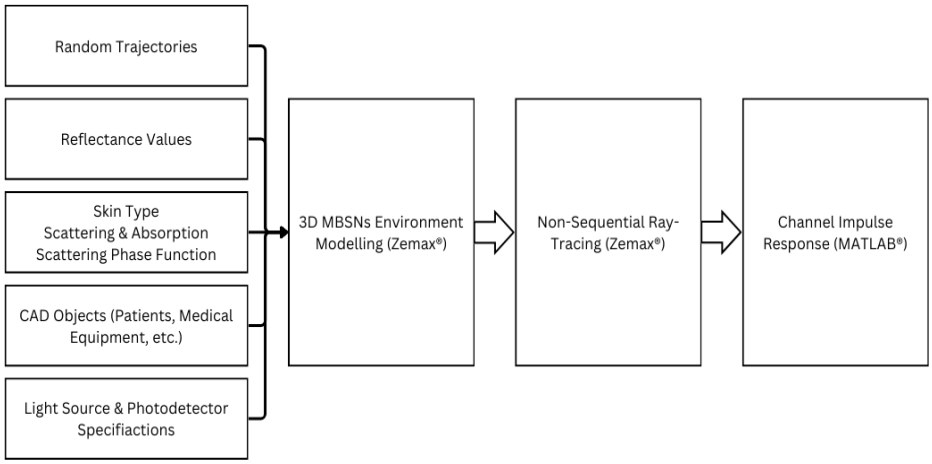

Figure 3.2: steps for site-specific channel modeling in VLC-based MBSNs (Antaki et al., 2025)

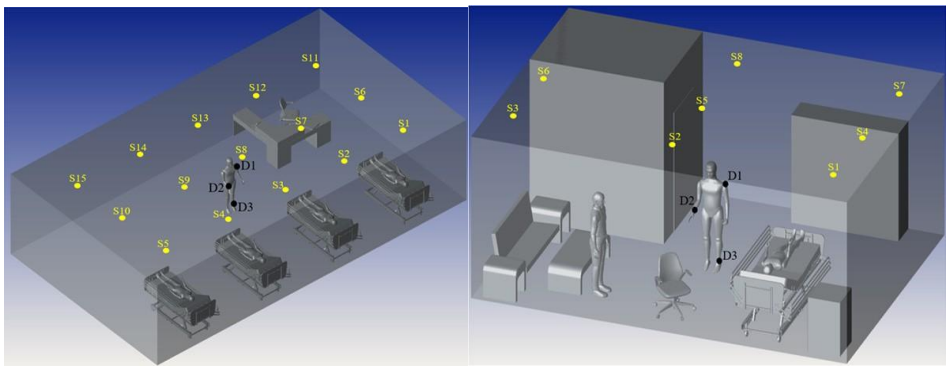

(a) (b)

Figure 3.3: Hospital Scenarios (a) ICU ward and (b) FTPR (Donmez & Miramirkhani, 2022)

Traditional channel modeling approaches often depend on basic mobility assumptions, such as random user locations, which might be acceptable for

infrared (IR)-based communication but fall short when applied to VLC systems. In the context of VLC-based MBSNs, it's crucial to represent realistic human mobility, as people don't move with fixed step lengths, follow only straight paths aligned to cardinal directions, or begin walking solely from doorway positions. To overcome these shortcomings, a more representative random trajectory model is adopted, capturing the natural flow of human movement. When combined with wavelength-sensitive channel modeling, this approach provides a more practical and accurate representation of dynamic VLC channels in clinical settings (Donmez & Miramirkhani, 2021). A random trajectory generator is used to simulate lifelike movement patterns for users in the chosen hospital environments. Although the current model is tailored for two specific hospital layouts, it is adaptable to a broader range of healthcare scenarios. The generated paths consist of multiple sample points, reflecting randomness in direction, stride length, and initial position. This methodology ensures that the model remains dependable under different movement behaviors and hospital configurations, making it suitable for diverse and realistic applications.

Robust approaches has been investigated to reduce the impacts of saturation in photodetector driven on by their exposure to different ambient light sources, including the sun and artificial illumination. For VLC systems under sun irradiation, the researchers of (Islim et al., 2018) employed bandpass optical blue filters in conjunction with adaptive bit, energy loading and direct current optical orthogonal frequency division multiplexing. Without optical filtering, the results demonstrated data rates reaching 1 Gb/s at 50350 lux of sun illumination. Additionally, employing commercially available blue filters improved the SNR ratio by at least 6.47 dB, making up around 50% of the decreased data rate. This method could be modified for our design to handle possible saturation effects of the photodetector and guarantee dependable operation under high ambient light levels.

Also, each launched photon's complete path distance and received power from a source to a PD are determined via ray tracing computations. MATLAB® (R2024b) is used to process these simulations to calculate CIRs as:

$$h(t) = \sum_{k=1}^{M} P_k \delta(t - t_k) \qquad (3.1)$$

Where P_k Is the k_{th} ray detected power, t_k is the travel duration, and M is the total number of collected rays.

After that, channel parameters are calculated. The channel DC gain which denotes the received total power, is described as:

$$H_0 = \int_0^{+\infty} h(t)dt \qquad (3.2)$$

Thereafter, the path loss is calculated by:

$$PL = -10\log_{10} H_0 \qquad (3.3)$$

Another channel characteristic parameter is the RMS delay spread, representing the delay standard deviation denoted by:

$$\tau_{RMS} = \frac{\sqrt{\int_0^{+\infty} (t - \tau_0)^2 \, h(t)dt}}{H_0} \qquad (3.4)$$

Where τ_0 denotes the mean excess delay.

Moreover, Comprehensive simulation investigations, as detailed in (Donmez & Miramirkhani, 2022), show that the log-normal distribution fits both path loss and RMS delay spread histograms properly, which was demonstrated by:

$$f(PL) = \frac{1}{PL\sigma\sqrt{2\pi}} e^{\left(-\frac{(\ln(PL)-\mu)^2}{2\sigma^2}\right)} \qquad (3.5)$$

$$f(\tau_{RMS}) = \frac{1}{\tau_{RMS}\sigma\sqrt{2\pi}} e^{\left(-\frac{(\ln(\tau_{RMS})-\mu)^2}{2\sigma^2}\right)} \qquad (3.6)$$

Where μ and σ denote location and scale parameters, respectively.

3.2.2 Lstm-Based Channel Parameter Estimation

The distinctive RNN type that is known as Long Short-Term Memory (LSTM) is constructed from input gate $i^{(t)}$, forget gate $f^{(t)}$, cell gate $c^{(t)}$, and output gate $o^{(t)}$ (Guo et al., 2022). This approach enables the user's mobile to anticipate random walks over random trajectories without sample points known. Figure 3.4 shows LSTM's complete architecture. Moreover, in contrast to conventional techniques, it can handle dynamic and complicated propagation situations with improved performance, adaptability, and predictability (Van Houdt et al., 2020).

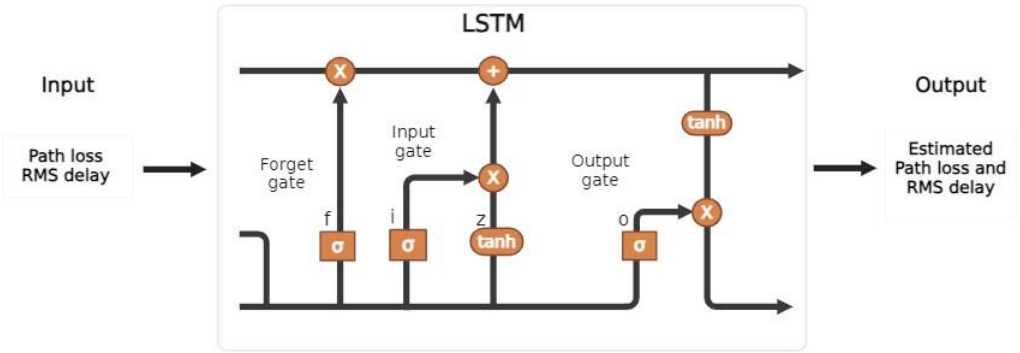

Figure 3.4: LSTM design architecture to estimate PL and τ_{RMS} in VLC-based MBSNs (Antaki et al., 2025)

When the data order points is important and strongly correlated, networks using LSTM perform exceptionally well. They can estimate future information points based on previous findings since they are made to progressively learn these relationships. This feature, along with their memory and gating mechanism, enables LSTMs to react to the constant oscillations of wireless channels and efficiently capture long-range temporal relationships. They are the perfect choice for mimicking dynamic channel scenarios and user mobility within VLC-based MBSNs because of their capacity to choose remain or forget information, even in situations with substantial variability over an extended period. The technique begins by modifying block input with the most recent output $y^{(t-1)}$ and the present input $x^{(t)}$ as :

$$z^{(t)} = g\left(W_z x^{(t)} + R_z y^{(t-1)} + b_z\right) \qquad (3.7)$$

Where the input, output, and bias weight vectors are represented by the weights W_z, R_z, and b_z, respectively. The data estimated is determined via the present cell value and the output gate in the form of:

$$y^{(t)} = g\left(c^{(t)}\right) \odot o^{(t)} \qquad (3.8)$$

Where g(x)=tanh(x) and $\odot$ is the two vector point-wise multiplication. Algorithm 1 provides the algorithmic details by determining the gradients required to modify the weights inside each gate. Table 3.3 displays the parameters of the LSTM's design.

Algorithm 1: ML-based Path Loss and RMS Delay Spread Estimation for VLC-based MBSNs

Data: Path loss (*PL*), and RMS delay spread (τ_{RMS})
Input : *PL* and τ_{RMS}
Output: Obtain the estimated $\hat{PL}$, and $\hat{\tau_{RMS}}$
while *true* **do**
  Pass PL and τ_{RMS} through ML gates
  while *In block input* $z^{(t)}$ **do**
    Update the block input based on the current information $x^{(t)}$ and previous output $y^{(t-1)}$
  while *In the input gate* $i^{(t)}$ **do**
    Revise $x^{(t)}$,$y^{(t-1)}$ and the previous cell value $c^{(t-1)}$
  while *In forget gate* $f^{(t)}$ **do**
    Decide which information should be removed using $x^{(t)}$,$y^{(t-1)}$ and $c^{(t-1)}$
  while *In the cell gate* $c^{(t)}$ **do**
    Compute $c^{(t)}$ based on $z^{(t)}$,$i^{(t)}$, $c^{(t-1)}$, and $f^{(t)}$
  while *In the output gate* $o^{(t)}$ **do**
    Calculate $o^{(t)}$ by $x^{(t)}$,$y^{(t-1)}$ and $c^{(t)}$
  while *In the block output* $y^{(t)}$ **do**
    Predict $y^{(t)}$ based on, g($c^{(t)}$), along with $o^{(t)}$
Modify each gate weights and estimate $\hat{PL}$, and $\hat{\tau_{RMS}}$
End

Table 3.3: LSTM design specifications (Antaki et al., 2025)

Parameters	Specifications
Optimizer	ADAM
Number of iterations	800
Learning Rate	0.001
Number of Epochs	400
Number of Hidden units	55

In addition, Root Mean Squared Error (RMSE) is considered a critical metric for evaluating the performance in regression tasks and sequence prediction within AI and machine learning since it is computed as the square root of the average squared differences between predicted and actual values. RMSE can be described as:

$$RMSE = \sqrt{\frac{1}{n}\sum_{j=1}^{n}\left(y_j - \hat{y}_j\right)^2} \qquad (3.9)$$

Where y_j, $\hat{y}_j$, and n represents the actual values, predicted values, and number of data points respectively. Moreover, RMSE values vary between 0 and positive infinity where low values illustrate accurate and good fit whereas high values express inaccurate and bad forecasts. Various metrics such as Mean Squared Error (MSE), Mean Absolute Error (MAE), and R-squared are relevant in evaluating the performance and accuracy of the algorithms however, RMSE is a robust metric that provides high sensitivity to outliers, interoperability, and ensures both consistency and comparability across different studies since it uses a standardized method to compare different algorithms along with calculates the measured error as the target variable unit as well as highlight larger discrepancies effectively.

The time complexity of the intended LSTM model may be calculated by taking input features (F), hidden units (H), and the effective batch size (B) while training. O(BH(F+H)) provides an approximate value for the total operations number carried out per iteration.

3.3 NUMERICAL RESULTS

The CIRs are found in the ICU ward and FTPR settings using a site-specific non-sequential ray tracing algorithm (Donmez et al., 2021). In both settings, the dependent wavelength reflectance, particular luminaries on the ceilings, and human body PDs were obtained using CAD objects. The luminaries are spaced out to guarantee the lowest average illumination level and minimum uniformity illuminance ratio. In order to create the MBSNs, three sensor detectors are affixed to the individual anatomy, with (D1) placed on the shoulder, (D2) on the wrist, and (D3) on the ankle (Donmez et al., 2021). The first scenario is an ICU ward setting consisting of four patients sleeping in beds, a desk, a chair, and a medical professional who walks randomly within the room. In addition, the second setting is an FTPR that includes a patient lying in bed, furniture, a medical professional who also considered walking randomly in the room, a sofa, and a bathroom. While the FTPR has dimensions of 7 m × 5 m × 3 m together with 8 luminaries, the ICU ward has room dimensions of 11.5 m × 6.5 m × 3 m along with 15 luminaries. Additionally, 20 randomly chosen trajectories with 10 consecutive points in both rooms are taken into account, with a uniform selection of step length and direction. Following random trajectory movement generation, the CIR provides path loss and RMS delay spread, which are then subjected to various machine learning methods in order to obtain PL and RMS delay spread estimation.

Through extensive simulation analysis utilizing a variety of ML methods, path loss and RMS spread of delay estimation for the three detectors D1–D3 within both ICU room ward and FTPR settings were determined. Tables 3.4 and Table 3.5 provide details on the observed Root Mean Squared Error (RMSE)

values for these particular cases. As shown in Figure 3.6 and Figure 3.7, the LSTM approach outperforms considered models across the two hospital scenarios, obtaining a lower RMSE for path loss and RMS spread. This illustrates how well LSTM performs in reducing prediction error.

In order to ensure the best outcomes from the LSTM model, specific procedures were applied to optimize performance with our datasets. First, smaller dataset files in CSV format were used, with an 80/20 split between training and validation sets. The data was reshaped for processing through the LSTM algorithm. Important preprocessing operations were carried out to enhance the stability of training and the performance of the approach, including normalization by computing the standard deviation and mean.

Table 3.4: Path loss and RMS delay estimation results in ICU using multiple approaches (Antaki et al., 2025)

Technique	ICU Ward					
	RMSE of PL (dB)			RMSE of τ_{RMS} (ns)		
	D1	D2	D3	D1	D2	D3
LSTM	1.6797	1.1679	1.1464	1.0567	0.9348	0.8784
GRU	1.7060	1.1808	1.1774	1.0794	0.9593	0.8840
RNN	1.7398	1.2647	1.1785	1.0904	0.9734	0.9039
Linear Regression	1.8269	1.3216	1.2161	1.2106	1.0067	0.9006
SVR	1.8470	1.3671	1.2654	1.1774	0.9769	0.9107
KNN	2.3142	1.8848	1.7834	1.8088	1.5987	1.4401

Table 3.5: Path loss and RMS delay estimation results in FTPR using multiple approaches (Antaki et al., 2025)

Technique	FTPR					
	RMSE of PL (dB)			RMSE of τ_{RMS} (ns)		
	D1	D2	D3	D1	D2	D3
LSTM	0.7210	0.7327	1.0652	0.5830	0.6230	0.7657
GRU	0.7359	0.7832	1.1480	0.6183	0.6352	0.8555
RNN	0.7663	0.7929	1.1886	0.6237	0.6509	0.8509
Linear Regression	0.7804	0.8158	1.1611	0.6246	0.6535	0.8705
SVR	0.7829	0.8184	1.1762	0.6277	0.6753	0.8834
KNN	0.9110	0.9770	1.7908	0.8199	0.9602	1.2166

The LSTM model was designed with 55 neurons in the hidden layer, balancing complexity and the capacity to represent patterns in the sequential data. While increasing the number of hidden units can capture more complex patterns, it also raises the risk of overfitting. Therefore, a moderated number of hidden layers was chosen to mitigate overfitting. A 0.4 dropout layer rate was used to avoid both underfitting and overfitting, and a 0.001 learning rate was applied to achieve accurate training. The Adam optimization technique was employed to control training speed, convergence, and generalization performance. The model was trained over 400 epochs to produce the simulation results. To ensure accuracy, RMSE was calculated before normalization and after denormalization. The normalized RMSE reflects the LSTM's performance over the training and validation sets, while the denormalized RMSE indicates validation accuracy results compared to the training set (Shu et al., 2024). Figure 3.5 shows the LSTM training step using a certain detector in the ICU ward setting.

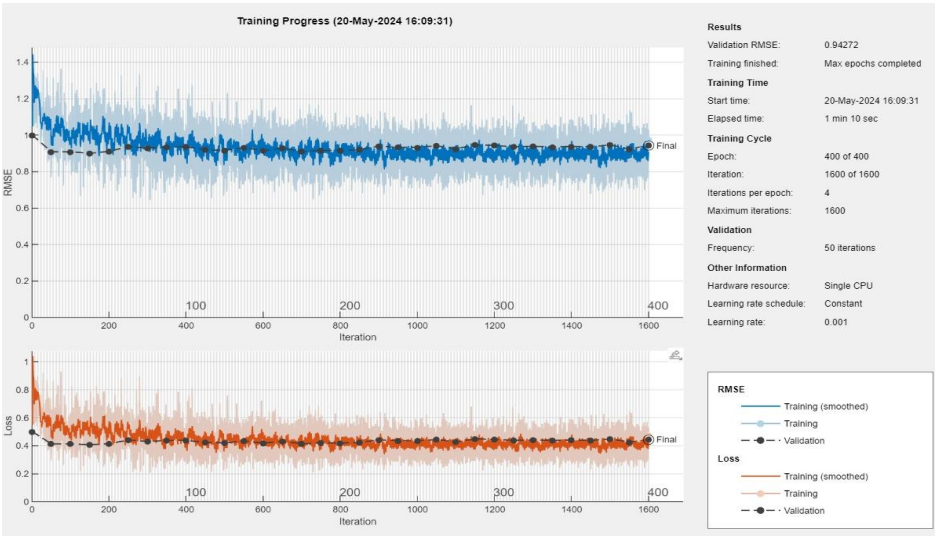

Figure 3.5: LSTM training step using D1 within the ICU ward (Dalloul et al., 2024)

As shown in Table 3.4, the LSTM model consistently delivers the lowest RMSE values for both PL and RMS delay spread across all detectors (D1–D3) within the ICU environment, clearly outperforming the other methods—GRU, standard RNN, SVR, KNN, and LR —which show progressively larger errors. In the ICU setting, LSTM reports RMSE values of 1.6797, 1.1679, and 1.1464 for PL at detectors D1, D2, and D3, respectively. GRU comes closest with slightly higher values of 1.7060, 1.1808, and 1.1774. Similarly, Table 3.5 reflects LSTM's continued advantage in the FTPR scenario, where it achieves PL RMSEs of 0.7210, 0.7327, and 1.0652 across D1 to D3, whereas GRU again follows with values of 0.7359, 0.7832, and 1.1480. For RMS delay spread, LSTM again takes the lead in the ICU ward, recording RMSEs of 1.0567, 0.9348, and 0.8784 at D1, D2, and D3, respectively—marginally ahead of GRU, which records 1.0794, 0.9593, and 0.8840 as shown in Table 3.4. In the FTPR case shown in Table 3.5, LSTM maintains its superiority with RMS spread RMSEs of 0.5830, 0.6230, and 0.7657, while GRU reports 0.6183, 0.6352, and 0.8555. Across both scenarios and both performance metrics, the rest of the models follow with increasingly higher RMSEs, reinforcing LSTM's position as the most accurate among the evaluated techniques.

Based on Table 3.4 findings within the ICU ward setting, the estimated path loss for D1 has the highest RMSE when contrasted with D2 and D3. This is consistent with the findings in (Donmez & Miramirkhani, 2022), which show that, due to larger variance leads to higher estimated RMSE, the log-normal distribution of D1 has the highest variance value of 0.0262 when compared to D2 and D3 with variances of 0.0176 and 0.0169, respectively. Additionally, according to Table 3.5, D3 has the largest RMSE within the FTPR room scenario when contrasted with D1 and D2, which supports the findings in (Donmez & Miramirkhani, 2022), where D3's log-normal distribution has the largest variance value of 0.0168 when contrasted to D1 and D2's variances of 0.0123 and 0.0119, respectively, due to the same fact that largest variance detector results in high RMSE estimated.

Additionally, Table 3.4 shows that the estimated RMS delay spread for D1 in the ICU ward setting has the greatest RMSE when contrasted with D2 and D3. This is due to the fact that D1's log-normal distribution, as determined in (Donmez & Miramirkhani, 2022), has the largest variance of 0.0975, whereas 0.0847 for D2 and 0.0780 for D3. Therefore, it refers to the same argument which states that a larger variance results in a bigger estimated RMSE. Nevertheless and according to Table 3.5, D3 has the largest RMSE when contrasted with D1 and D2, which supports the findings in (Donmez & Miramirkhani, 2022). The log-normal distribution of D3 has the greatest variance of 0.0967 when contrasted to both D1 and D2, which have variances of 0.0659 and 0.0747, respectively. This demonstrates that the greater variance values result in large RMSE estimated.

Furthermore, in order to validate our choice of LSTM, a time complexity investigation is presented, analyzing both training and prediction periods in the ICU ward and FTPR scenarios, as shown in Tables 3.6 and Table 3.7. The emphasis is on LSTM, GRU, and RNN due to their wide adoption within MBSN applications. These models are intended for sequential data regression problems which specialize in detecting temporal dependencies, thus rendering them ideal for time-series forecasting and real-time monitoring of health. As a result, they are frequently employed for tasks demanding accurate and effective MBSN system predictions.

According to Table 3.6, LSTM surpasses GRU and RNN on the execution time basis for D1-D3 across both PL and RMS distribution in the ICU ward, confirming the choice of LSTM. Likewise, according to Table 3.7, the evaluation's findings show that LSTM is preferred in the FTPR for D1-D3 when it comes to execution time for the PL and the RMS spread.

According to Table 3.6, LSTM performs better than RNN and GRU within the ICU ward setting in terms of D1-D3 execution time throughout PL and RMS delay spread, supporting our decision in favor of LSTM. The ICU ward's RMS delay spread execution durations were 69.946 s, 68.786 s, and 68.948 s, respectively, whereas the execution times for D1-D3 PL were 68.051

s, 65.854 s, and 66.229 s, respectively. In a similar manner the analytical findings show that LSTM is also favored in the FTPR setting for D1–D3 in terms of execution time for PL and RMS delay spread (Table 3.7). 69.112 s, 70.484 s, and 69.919 s were the execution times for D1-D3 PL in the FTPR, while 69.740 s, 70.220 s, and 69.650 s were the execution times for the RMS delay spread.

These outcomes are in line with our predictions since the structure of LSTM is adequate for VLC-based MBSN PL and RMS delay data due to its substantial memory, cell states, and capacity of capturing long sequential correlations. The resulted RMSE was comparatively near to other approaches like GRU however, our design accomplished low level of complexity, slight parameter adjustment, and faster training periods compared to other algorithms while maintaining the exact standard practices. The performance of LSTM shows a better fit to the complex temporal dependencies in our data, confirming its status as the most efficient and trustworthy model for our purposes.

LSTM models encounter real-world difficulties when used within healthcare settings, such as consumption of energy, integrating systems, complexity, and the healthcare setting nature. In order to tackle these issues, the researchers in (A. K. Saxena et al., 2022) used LSTM to analyze real-time and historical data within two resource allocation scenarios in order to improve Hospital Management Systems performance. The residual errors of the model were close to zero, indicating a strong agreement between the expected and actual results. On the other hand, LSTM was employed by the authors of (Karsanti et al., 2019) to forecast patient visits of a community health center using historical data of 43 months. LSTM did better than the other models, as seen by its 4.714 Mean Absolute Percentage Error (MAPE),154.796 MAE, and 167.631 RMSE. This suggests that the LSTM framework can adjust to changing conditions while retaining a high level of operational accuracy and resilience. Additionally, the findings imply that the model's capacity to effectively understand temporal patterns can reduce difficulties like computational complexity.

These results demonstrate how LSTM models can be used to address important issues in actual hospital settings, such as cutting down on wait times for patients, optimizing staff scheduling, and increasing patient outcomes in general.

Table 3.6: ICU ward time complexity (Antaki et al., 2025)

Technique	ICU Ward					
	Execution time of PL (s)			Execution time of τ_{RMS} (s)		
	D1	D2	D3	D1	D2	D3
LSTM	68.051	65.854	66.229	69.946	68.786	68.948
GRU	70.197	72.190	68.958	72.711	69.671	73.468
RNN	70.368	72.578	73.488	73.018	72.917	73.787

Table 3.7: FTPR time complexity (Antaki et al., 2025)

Technique	FTPR					
	Execution time of PL (s)			Execution time of τ_{RMS} (s)		
	D1	D2	D3	D1	D2	D3
LSTM	69.112	70.484	69.919	69.740	70.220	69.650
GRU	72.531	71.791	70.652	70.491	71.849	70.650
RNN	73.353	72.299	71.616	71.625	73.173	75.559

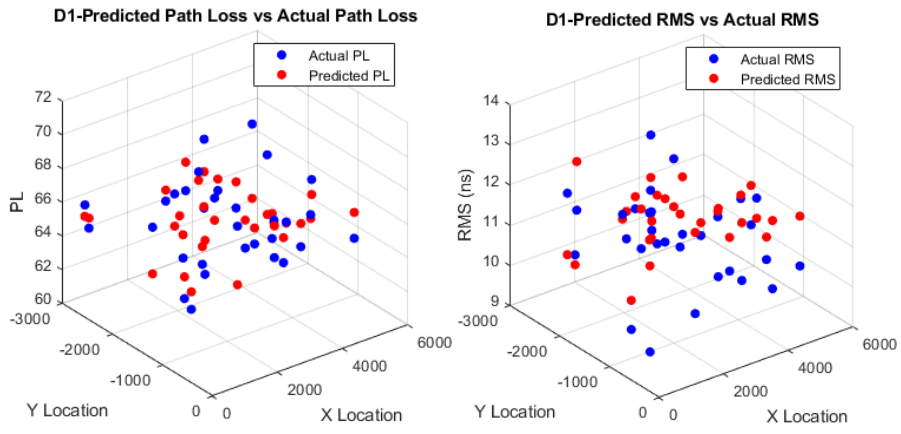

(a) (b)

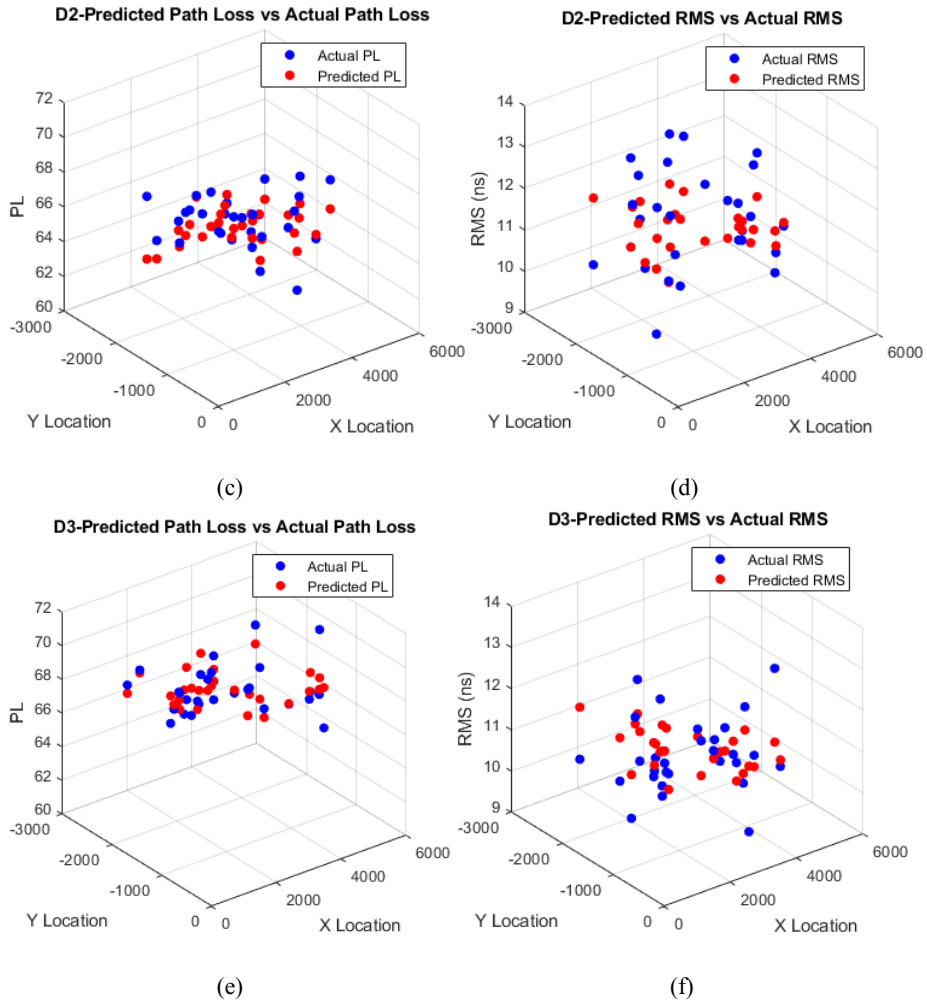

Figure 3.6: Estimated path loss (a,c,e) and RMS delay distribution (b,d,f) in ICU ward (Antaki et al., 2025)

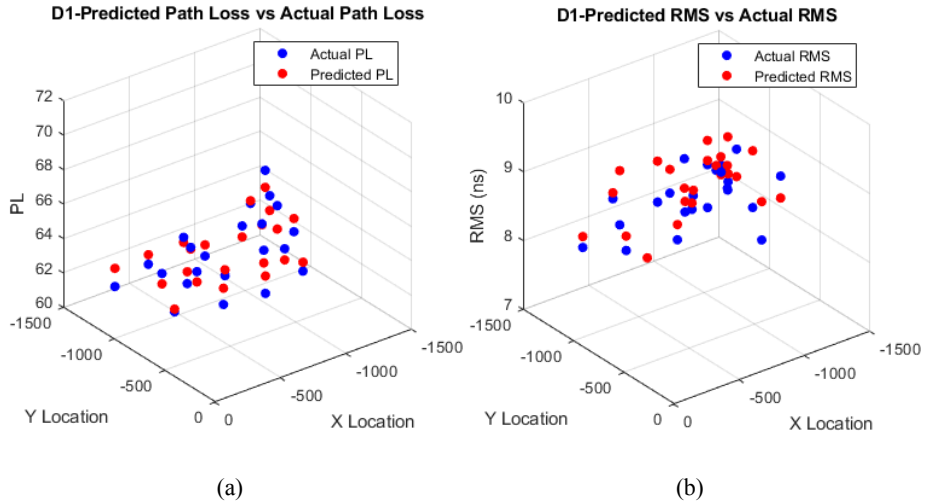

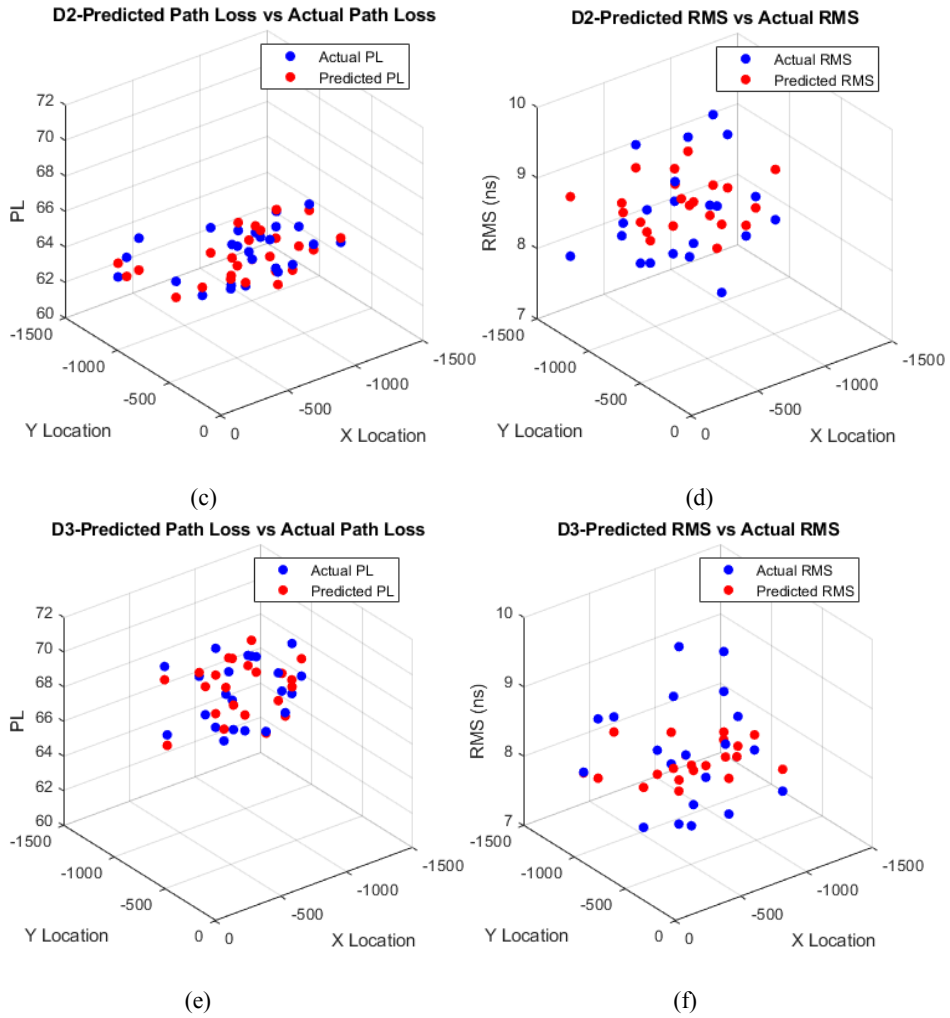

Figure 3.7: Estimated path loss (a,c,e) and RMS delay distribution (b,d,f) in FTPR (Antaki et al., 2025)

CHAPTER 4

4. POTENITOAN FUTURE DIRECTIONS

In recent years, health monitoring systems have undergone significant innovation, propelled by advances in wireless communication, ML, and sensor technologies. From wearable devices to intelligent remote monitoring platforms, these systems have greatly enhanced our capacity to detect health anomalies and deliver timely interventions. However, as research advances toward the integration of novel paradigms such as VLC and intelligent channel modeling, it becomes imperative to reassess and broaden the outlook for future development. Rather than limiting the scope to healthcare applications alone, future directions must also consider the technical, ethical, and deployment challenges of VLC-based MBSNs, especially in dynamic environments. This section explores the key areas where further research is needed to ensure that such systems become more robust, secure, and adaptable—ultimately paving the way for next-generation, intelligent health monitoring solutions.

- **Practical Deployment and Ethical Compliance in Healthcare:**

Future research must address practical and ethical concerns related to deploying MBSNs in hospital environments. The physical and electromagnetic complexities of healthcare settings such as multi-user interference, require further investigation and optimized channel coding techniques to enhance system robustness. Additionally, the use of IoT-enabled systems in healthcare introduces serious ethical concerns, particularly in maintaining informed consent, data privacy, and access control.

VLC-based MBSNs can contribute to mitigating some of these concerns, however, more practical research and overviews is required to develop standardized, robust secure, and privacy-compliant communication frameworks for medical applications.

- **Photodetector Saturation in Ambient Light Environments:**

One of the challenges of implementing VLC in real-world environments is the susceptibility of photodetectors to saturation from ambient light sources such as artificial lighting and sunlight. Although certain optical filtering techniques and adaptive modulation schemes have shown promise in mitigating these effects, their integration within mobile healthcare scenarios remains slightly underexplored. Future studies should investigate real-time compensation strategies that can dynamically adapt to varying ambient lighting conditions to maintain consistent communication quality and avoid signal distortion or loss.

- **Real-Time ML Challenges in Healthcare Settings:**

Implementing ML models like LSTM in hospital environments presents multiple challenges beyond algorithmic accuracy. These include computational constraints, energy efficiency, system integration with existing hospital infrastructure, and model responsiveness under dynamic operational conditions. While LSTM has demonstrated strong potential for modeling complex temporal dependencies, practical concerns such as latency, scalability, and hardware limitations must be rigorously addressed. Future work should focus on developing lightweight, interpretable, and hardware-efficient ML frameworks tailored for deployment in resource-constrained edge devices.

CONCLUSION AND DISCUSSION

Recent advances in the field of seamless medical monitoring devices have been reviewed within this thesis, covering a wide range of topics including antenna architecture, tiny embedded antennas, wearable devices that monitor the body, and adaptable detection and imaging technologies. We have conducted an extensive investigation into methods used in monitoring systems, which includes investigations on modern sensing and imaging techniques, wireless capsule endoscopic improvements, and channel characteristics. These developments highlight how individualized treatment plans, early intervention, and preventative care could be made possible by remote health monitoring devices, ultimately revolutionizing the healthcare industry.

Furthermore, this dissertation offers real statistical frameworks within hospital scenarios for channel modeling, as well as ML-based techniques for assessing path loss and RMS spread in VLC-enabled MBSNs. These frameworks take into consideration actual hospital environments, real random pathways, and wavelength dependency. According to detailed simulation assessments, D1 has the largest RMSE for estimated path loss (1.6797 dB) and RMS spread (1.0567 ns) under the ICU ward scenario, while D3 has the greatest RMSE for estimated path loss (1.0652 dB) and RMS spread (0.7657 ns) within the FTPR setting.

A precise assessment of VLC channel factors, including DC channel gain and RMS delay spread, is vital for resilient communication networks. We show that the placement of the photodetector and the geometry of the scenario have a significant impact on the ML-based technique performance for estimating such factors within VLC-based MBSNs. In order to improve both efficiency and reliability, such essential variables need to be taken into account while modeling VLC channels.

REFERENCES

Abdellatif, A. A., Mhaisen, N., Mohamed, A., Erbad, A., & Guizani, M. (2023). Reinforcement Learning for Intelligent Healthcare Systems: A Review of Challenges, Applications, and Open Research Issues. *IEEE Internet of Things Journal*, 1. https://doi.org/10.1109/JIOT.2023.3288050

Aggarwal, K., Joshi, K. R., Rajavi, Y., Taghivand, M., Pauly, J. M., Poon, A. S. Y., & Scott, G. (2017). A Millimeter-Wave Digital Link for Wireless MRI. *IEEE Transactions on Medical Imaging*, *36*(2), 574–583. https://doi.org/10.1109/TMI.2016.2622251

Albahri, A. S., Albahri, O. S., Zaidan, A. A., Zaidan, B. B., Hashim, M., Alsalem, M. A., Mohsin, A. H., Mohammed, K. I., Alamoodi, A. H., Enaizan, O., Nidhal, S., Zughoul, O., Momani, F., Chyad, M. A., Abdulkareem, K. H., Dawood, K. A., Almahdi, E. M., Al Shafeey, G. A., & Baqer, M. J. (2019). Based Multiple Heterogeneous Wearable Sensors: A Smart Real-Time Health Monitoring Structured for Hospitals Distributor. *IEEE Access*, *7*, 37269–37323. https://doi.org/10.1109/ACCESS.2019.2898214

Alibakhshikenari, M., Virdee, B. S., Shukla, P., Parchin, N. O., Azpilicueta, L., See, C. H., Abd-Alhameed, R. A., Falcone, F., Huynen, I., Denidni, T. A., & Limiti, E. (2020). Metamaterial-Inspired Antenna Array for Application in Microwave Breast Imaging Systems for Tumor Detection. *IEEE Access*, *8*, 174667–174678. https://doi.org/10.1109/ACCESS.2020.3025672

Alkandari, Y., Ijaz, M., Ekpo, S., Adebisi, B., Soto, I., Zamorano-Illanes, R., & Azurdia, C. (2023). Optimization of Visible Light Positioning in Industrial Applications using Machine Learning. *2023 South American Conference On Visible Light Communications (SACVLC)*, 141–146. https://doi.org/10.1109/SACVLC59022.2023.10347641

Antaki, B., Dalloul, A. H., & Miramirkhani, F. (2025). Intelligent Health Monitoring in 6G Networks: Machine Learning-Enhanced VLC-Based

Medical Body Sensor Networks. *Sensors*, *25*(11). https://doi.org/10.3390/s25113280

Ashok, K., & Gopikrishnan, S. (2023). Statistical Analysis of Remote Health Monitoring Based IoT Security Models & Deployments From a Pragmatic Perspective. *IEEE Access*, *11*, 2621–2651. https://doi.org/10.1109/ACCESS.2023.3234632

Bharadwaj, R., Swaisaenyakorn, S., Parini, C. G., Batchelor, J., & Alomainy, A. (2014). Localization of Wearable Ultrawideband Antennas for Motion Capture Applications. *IEEE Antennas and Wireless Propagation Letters*, *13*, 507–510. https://doi.org/10.1109/LAWP.2014.2309977

Boric-Lubecke, O., Gao, X., Yavari, E., Baboli, M., Singh, A., & Lubecke, V. M. (2014). E-healthcare: Remote monitoring, privacy, and security. *2014 IEEE MTT-S International Microwave Symposium (IMS2014)*, 1–3. https://doi.org/10.1109/MWSYM.2014.6848602

Boyle, J. (2006). Wireless Technologies and Patient Safety in Hospitals. *Telemedicine and E-Health*, *12*(3), 373–382. https://doi.org/10.1089/tmj.2006.12.373

Brandão Lent, D. M., Novaes, M. P., Carvalho, L. F., Lloret, J., Rodrigues, J. J. P. C., & Proença, M. L. (2022). A Gated Recurrent Unit Deep Learning Model to Detect and Mitigate Distributed Denial of Service and Portscan Attacks. *IEEE Access*, *10*, 73229–73242. https://doi.org/10.1109/ACCESS.2022.3190008

Buke, A., Gaoli, F., Yongcai, W., Lei, S., & Zhiqi, Y. (2015). Healthcare algorithms by wearable inertial sensors: a survey. *China Communications*, *12*(4), 1–12. https://doi.org/10.1109/CC.2015.7114054

Camli, B., Kusakci, E., Lafci, B., Salman, S., Torun, H., & Yalcinkaya, A. D. (2017). Cost-Effective, Microstrip Antenna Driven Ring Resonator Microwave Biosensor for Biospecific Detection of Glucose. *IEEE Journal of*

Selected Topics in Quantum Electronics, *23*(2), 404–409. https://doi.org/10.1109/JSTQE.2017.2659226

Celik, A., & Eltawil, A. M. (2022). The Internet of Bodies: The Human Body as an Efficient and Secure Wireless Channel. *IEEE Internet of Things Magazine*, *5*(3), 114–120. https://doi.org/10.1109/IOTM.001.2100209

Celik, A., Salama, K. N., & Eltawil, A. M. (2022). The Internet of Bodies: A Systematic Survey on Propagation Characterization and Channel Modeling. *IEEE Internet of Things Journal*, *9*(1), 321–345. https://doi.org/10.1109/JIOT.2021.3098028

Chu, H., Wang, P.-J., Zhu, X.-H., & Hong, H. (2019). Antenna-in-Package Design and Robust Test for the Link Between Wireless Ingestible Capsule and Smart Phone. *IEEE Access*, *7*, 35231–35241. https://doi.org/10.1109/ACCESS.2019.2891880

Čibiraitė-Lukenskienė, D., Ikamas, K., Lisauskas, T., Krozer, V., Roskos, H. G., & Lisauskas, A. (2020). Passive Detection and Imaging of Human Body Radiation Using an Uncooled Field-Effect Transistor-Based THz Detector. *Sensors*, *20*(15). https://doi.org/10.3390/s20154087

Cui, W., Liu, R., Wang, L., Wang, M., Zheng, H., & Li, E. (2019). Design of Wideband Implantable Antenna for Wireless Capsule Endoscope System. *IEEE Antennas and Wireless Propagation Letters*, *18*(12), 2706–2710. https://doi.org/10.1109/LAWP.2019.2949630

Dalloul, A. H., Miramirkhani, F., & Kouhalvandi, L. (2023). A Review of Recent Innovations in Remote Health Monitoring. *Micromachines*, *14*(12). https://doi.org/10.3390/mi14122157

Donmez, B., & Miramirkhani, F. (2021). Channel Modeling and Characterization for VLC-based MBSNs Impaired by 3D User Mobility. *2021 13th International Conference on Electrical and Electronics Engineering (ELECO)*, 485–489.

Donmez, B., & Miramirkhani, F. (2022). Path Loss and RMS Delay Spread Model for VLC-based Patient Health Monitoring System. *2022 4th West Asian Symposium on Optical and Millimeter-Wave Wireless Communications (WASOWC)*, 1–5. https://doi.org/10.1109/WASOWC54657.2022.9798434

Donmez, B., Mitra, R., & Miramirkhani, F. (2021). Channel modeling and characterization for VLC-based medical body sensor networks: trends and challenges. *IEEE Access*, *9*, 153401–153419.

Du, P., Zhang, S., Alphones, A., & Chen, C. (2021). Faster Deployment for Indoor Visible Light Positioning Using Xgboost Algorithms in Industrial Internet-of-Things. *IECON 2021 – 47th Annual Conference of the IEEE Industrial Electronics Society*, 1–7. https://doi.org/10.1109/IECON48115.2021.9589151

Elayan, H., Shubair, R. M., Jornet, J. M., & Johari, P. (2017). Terahertz Channel Model and Link Budget Analysis for Intrabody Nanoscale Communication. *IEEE Transactions on NanoBioscience*, *16*(6), 491–503. https://doi.org/10.1109/TNB.2017.2718967

Fawole, O. C., & Tabib-Azar, M. (2016). Terahertz Near-Field Imaging of Biological Samples With Horn Antenna-Excited Probes. *IEEE Sensors Journal*, *16*(24), 8752–8760. https://doi.org/10.1109/JSEN.2016.2582387

Fei Chengwei and Liu, R. and L. Z. and W. T. and B. F. N. (2021). Machine and Deep Learning Algorithms for Wearable Health Monitoring. In S. and S. M. and P. S. Manocha Amit Kumar and Jain (Ed.), *Computational Intelligence in Healthcare* (pp. 105–160). Springer International Publishing. https://doi.org/10.1007/978-3-030-68723-6_6

Floor, P. A., Chávez-Santiago, R., Kim, A. N., Kansanen, K., Ramstad, T. A., & Balasingham, I. (2019). Communication Aspects for a Measurement Based UWB in-Body to on-Body Channel. *IEEE Access*, *7*, 29425–29440. https://doi.org/10.1109/ACCESS.2019.2902104

Gabor, A., & Gausz, B. (2018). 10.3 Case Study—Remote Health Monitoring with Wearable Sensors and Smartphones. *Co-Production and Co-Creation*, 134.

Gahlot, S., Reddy, S. R. N., & Kumar, D. (2019). Review of Smart Health Monitoring Approaches With Survey Analysis and Proposed Framework. *IEEE Internet of Things Journal*, *6*(2), 2116–2127. https://doi.org/10.1109/JIOT.2018.2872389

Gizzini, A. K., & Chafii, M. (2024). RNN Based Channel Estimation in Doubly Selective Environments. *IEEE Transactions on Machine Learning in Communications and Networking*, *2*, 1–18. https://doi.org/10.1109/TMLCN.2023.3332021

Gu, Z., Yang, J., & Wang, P. (2024*).* Research on channel modeling technology of visible light communication system based on the ray tracing method. *Journal of Physics: Conference Series*, *2807*(1), 12043. https://doi.org/10.1088/1742-6596/2807/1/012043

Guaña-Moya, J., Román Cañizares, M., Palacios Játiva, P., Sánchez, I., Ruminot, D., & Lobos, F. V. (2024). Comprehensive Survey on VLC in E-Healthcare: Channel Coding Schemes and Modulation Techniques. *Applied Sciences*, *14*(19). https://doi.org/10.3390/app14198912

Guo, J., Zhang, Q., Zhao, Y., Shi, H., Jiang, Y., & Sun, J. (2022). RNN-Test: Towards Adversarial Testing for Recurrent Neural Network Systems. *IEEE Transactions on Software Engineering*, *48*(10), 4167–4180. https://doi.org/10.1109/TSE.2021.3114353

Hassan, N. M., Olaniyi, O. M., Ahmed, A., & Dogo, E. M. (2013). Wireless sensor networks for remote healthcare monitoring in Nigeria: Challenges and way forward. *2013 IEEE International Conference on Emerging and Sustainable Technologies for Power and ICT in a Developing Society (NIGERCON)*, 182–187. https://doi.org/10.1109/NIGERCON.2013.6715654

Hwang, J. H., Kang, T. W., Park, S. O., & Kim, Y. T. (2015). Empirical Channel Model for Human Body Communication. *IEEE Antennas and Wireless Propagation Letters*, *14*, 694–697. https://doi.org/10.1109/LAWP.2014.2377051

Ishida, K., Wu, I., Gototh, K., & Matsumoto, Y. (2020). Electromagnetic compatibility of 400 MHz radio communications in hospitals: Safety management of wireless medical telemetry. *Journal of Medical Systems*, 44, 1–9.

Islim, M. S., Videv, S., Safari, M., Xie, E., McKendry, J. J. D., Gu, E., Dawson, M. D., & Haas, H. (2018). The Impact of Solar Irradiance on Visible Light Communications. *Journal of Lightwave Technology*, *36*(12), 2376–2386. https://doi.org/10.1109/JLT.2018.2813396

Játiva, P. P., Becerra, R., Azurdia-Meza, C. A., Zabala-Blanco, D., Soto, I., & Cañizares, M. R. (2021). Extreme Learning Machine Based Channel Estimator and Equalizer for Underground Mining VLC Systems. *2021 IEEE Latin-American Conference on Communications (LATINCOM)*, 1–6. https://doi.org/10.1109/LATINCOM53176.2021.9647737

Jia, Y., Guler, U., Lai, Y.-P., Gong, Y., Weber, A., Li, W., & Ghovanloo, M. (2020). A Trimodal Wireless Implantable Neural Interface System-on-Chip. *IEEE Transactions on Biomedical Circuits and Systems*, *14*(6), 1207–1217. https://doi.org/10.1109/TBCAS.2020.3037452

Junior, A. P., Díez, L. E., Bahillo, A., & Eyobu, O. S. (2023). Remote Pedestrian Localization Systems for Resource-Constrained Environments: A Systematic Review. *IEEE Access*, *11*, 36865–36889. https://doi.org/10.1109/ACCESS.2023.3266957

K, S., Kripesh, E., & Menon, K. (2016). A survey of remote patient monitoring systems for the measurement of multiple physiological parameters. *Health and Technology*, *7*. https://doi.org/10.1007/s12553-016-0171-1

Karsanti, H. T., Ardiyanto, I., & Nugroho, L. E. (2019). Deep Learning-Based Patient Visits Forecasting Using Long Short Term Memory. *2019 International Conference of Artificial Intelligence and Information Technology (ICAIIT)*, 344–349. https://doi.org/10.1109/ICAIIT.2019.8834634

Khaleghi, A., Hasanvand, A., & Balasingham, I. (2019). Radio Frequency Backscatter Communication for High Data Rate Deep Implants. *IEEE Transactions on Microwave Theory and Techniques*, *67*(3), 1093–1106. https://doi.org/10.1109/TMTT.2018.2886844

Khan, U., Ye, Y., Aisha, A.-U., Swar, P., & Pahlavan, K. (2018). Precision of EM Simulation Based Wireless Location Estimation in Multi-Sensor Capsule Endoscopy. *IEEE Journal of Translational Engineering in Health and Medicine*, *6*, 1–11. https://doi.org/10.1109/JTEHM.2018.2818177

King, C. E., & Sarrafzadeh, M. (2018). A survey of smartwatches in remote health monitoring. *Journal of Healthcare Informatics Research*, *2*, 1–24.

Kocabas, O., Soyata, T., & Aktas, M. K. (2016). Emerging Security Mechanisms for Medical Cyber Physical Systems. *IEEE/ACM Transactions on Computational Biology and Bioinformatics*, *13*(3), 401–416. https://doi.org/10.1109/TCBB.2016.2520933

Koutsoupidou, M., Cano-Garcia, H., Pricci, R. L., Saha, S. C., Palikaras, G., Kallos, E., & Kosmas, P. (2020). Study and Suppression of Multipath Signals in a Non-Invasive Millimeter Wave Transmission Glucose-Sensing System. *IEEE Journal of Electromagnetics, RF and Microwaves in Medicine and Biology*, *4*(3), 187–193. https://doi.org/10.1109/JERM.2019.2938876

Krishna, C., Kumar, D., & Kushwaha, D. S. (2023). A Comprehensive Survey on Pandemic Patient Monitoring System: Enabling Technologies, Opportunities, and Research Challenges. *Wireless Personal Communications*, 1–48.

Kuila, C., Maji, A., Murmu, N. C., Kuila, T., & Srivastava, S. K. (2023). Recent advancements in carbonaceous nanomaterials for multifunctional broadband electromagnetic interference shielding and wearable devices. *Carbon*, *210*, 118075. https://doi.org/https://doi.org/10.1016/j.carbon.2023.118075

Lea, A., Hui, P., Ollikainen, J., & Vaughan, R. G. (2009). Propagation Between On-Body Antennas. *IEEE Transactions on Antennas and Propagation*, *57*(11), 3619–3627. https://doi.org/10.1109/TAP.2009.2031917

Lee, S. H., Lee, J., Yoon, Y. J., Park, S., Cheon, C., Kim, K., & Nam, S. (2011). A Wideband Spiral Antenna for Ingestible Capsule Endoscope Systems: Experimental Results in a Human Phantom and a Pig. *IEEE Transactions on Biomedical Engineering*, *58*(6), 1734–1741. https://doi.org/10.1109/TBME.2011.2112659

Li, Y., Luo, J., Li, X., Pu, M., Ma, X., Xie, X., Shi, J., & Luo, X. (2020). Switchable Quarter-Wave Plate and Half-Wave Plate Based on Phase-Change Metasurface. *IEEE Photonics Journal*, *12*(2), 1–10. https://doi.org/10.1109/JPHOT.2020.2971592

Ma, P., Lin, H., Wang, W., Yu, H., Chen, F., Jiang, L., Zhou, L., Zhang, Z., Shi, G., & Wang, J. (2022). Toward Fine Surveillance: A review of multitemporal interferometric synthetic aperture radar for infrastructure health monitoring. *IEEE Geoscience and Remote Sensing Magazine*, *10*(1), 207–230. https://doi.org/10.1109/MGRS.2021.3098182

Ma, Z., Jia, P., Han, D., Zhang, M., Ghassemlooy, Z., & Wang, L. (2022). Deep-Learning-Based Channel Estimation for Multi-wavelength Visible Light Communication System. *2022 4th West Asian Symposium on Optical and Millimeter-Wave Wireless Communications (WASOWC)*, 1–4. https://doi.org/10.1109/WASOWC54657.2022.9798444

Maity, S., Jiang, X., & Sen, S. (2019). Theoretical Analysis of AM and FM Interference Robustness of Integrating DDR Receiver for Human Body Communication. *IEEE Transactions on Biomedical Circuits and Systems*, *13*(3), 566–578. https://doi.org/10.1109/TBCAS.2019.2911475

Manikandan, R., Arunprakash, S., Alsowail, R. A., & Pandiaraj, T. (2025). A novel wireless sensor network deployment for monitoring and predicting abnormal actions in medical environment and patient health state. *Alexandria Engineering Journal*, *119*, 149–167. https://doi.org/https://doi.org/10.1016/j.aej.2025.01.064

Mao, S., & Sejdić, E. (2023). A Review of Recurrent Neural Network-Based Methods in Computational Physiology. *IEEE Transactions on Neural Networks and Learning Systems*, *34*(10), 6983–7003. https://doi.org/10.1109/TNNLS.2022.3145365

Marzencki, M., Lin, P., Cho, T., Guo, J., Ngai, B., & Kaminska, B. (2011). Remote health, activity, and asset monitoring with wireless sensor networks. *2011 IEEE 13th International Conference on E-Health Networking, Applications and Services*, 98–101. https://doi.org/10.1109/HEALTH.2011.6026796

Maulud, D., & Abdulazeez, A. M. (2020). A review on linear regression comprehensive in machine learning. *Journal of Applied Science and Technology Trends*, *1*(2), 140–147.

Mia, Md. M. H., Mahfuz, N., Habib, Md. R., & Hossain, R. (2021). An Internet of Things Application on Continuous Remote Patient Monitoring and Diagnosis. *2021 4th International Conference on Bio-Engineering for Smart Technologies (BioSMART)*, 1–6. https://doi.org/10.1109/BioSMART54244.2021.9677715

Mitra, P., Bhattacharjee, R., Chatterjee, T., De, S., Karmakar, R., Ghosh, A., & Adhikari, T. (2021). Towards 6G Communications: Architecture, Challenges, and Future Directions. *2021 12th International Conference on Computing Communication and Networking Technologies (ICCCNT)*, 1–7. https://doi.org/10.1109/ICCCNT51525.2021.9580084

Mitra, R., & Kaddoum, G. (2022). Random Fourier Feature-Based Deep Learning for Wireless Communications. *IEEE Transactions on Cognitive Communications and Networking*, *8*(2), 468–479. https://doi.org/10.1109/TCCN.2022.3164898

Mollah, Md. A., Sarker, H., Ahsan, M., Elahi, Md. T., Based, Md. A., Haider, J., & Palani, S. (2021). Designing Highly Sensitive Surface Plasmon Resonance Sensor With Dual Analyte Channels. *IEEE Access*, *9*, 139293–139302. https://doi.org/10.1109/ACCESS.2021.3118927

Montaseri, N., Khodkar, Z., Abouei, J., Whittow, W. G., & Plataniotis, K. N. (2023). A Conformal Leaky-Wave Antenna Design for IoMT-based WBANs. *IEEE Access*, 1. https://doi.org/10.1109/ACCESS.2023.3274741

Mshali, H., Lemlouma, T., Moloney, M., & Magoni, D. (2018). A survey on health monitoring systems for health smart homes. *International Journal of Industrial Ergonomics*, *66*, 26–56.

Naser, S., Bariah, L., Muhaidat, S., Sofotasios, P. C., Al-Qutayri, M., Damiani, E., & Debbah, M. (2022). Toward Federated-Learning-Enabled Visible Light Communication in 6G Systems. *IEEE Wireless Communications*, *29*(1), 48–56. https://doi.org/10.1109/MWC.005.00334

Niarchou, E., Boucouvalas, A. C., Ghassemlooy, Z., Alves, L. N., & Zvanovec, S. (2021). Visible Light Communications for 6G Wireless Networks. *2021 Third South American Colloquium on Visible Light Communications (SACVLC)*, 1–6. https://doi.org/10.1109/SACVLC53127.2021.9652231

Nikolayev, D., Zhadobov, M., Le Coq, L., Karban, P., & Sauleau, R. (2017). Robust Ultraminiature Capsule Antenna for Ingestible and Implantable Applications. *IEEE Transactions on Antennas and Propagation*, *65*(11), 6107–6119. https://doi.org/10.1109/TAP.2017.2755764

Oesterling, A. X., Imani, M. F., Mizrahi, O. S., Gollub, J. N., & Smith, D. R. (2020). Detecting Motion in a Room Using a Dynamic Metasurface Antenna. *IEEE Access*, *8*, 222496–222505. https://doi.org/10.1109/ACCESS.2020.3043206

Oh, S. M., Nair, S., Casler, A., Nguyen, D., Forero, J. P., Joco, C., Kubert, J., Esses, D., Adams, D., Jariwala, S., & others. (2022). A prospective observational study evaluating the use of remote patient monitoring in ED discharged COVID-19 patients in NYC. *The American Journal of Emergency Medicine*, *55*, 64–71.

Omer, A. E., Gigoyan, S., Shaker, G., & Safavi-Naeini, S. (2020). WGM-Based Sensing of Characterized Glucose- Aqueous Solutions at mm-Waves. *IEEE Access*, *8*, 38809–38825. https://doi.org/10.1109/ACCESS.2020.2975805

Peng, Y., Saito, K., & Ito, K. (2018). Antenna Design for Impulse-Radio-Based Wireless Capsule Endoscope Communication Systems. *IEEE Transactions on Antennas and Propagation*, *66*(10), 5031–5042. https://doi.org/10.1109/TAP.2018.2854360

Periyasam, M., & Dhanasekaran, R. (2013). Electromagnetic interference on critical medical equipments by RF devices. *2013 International Conference on Communication and Signal Processing*, 78–82. https://doi.org/10.1109/iccsp.2013.6577019

Petković, M. (2009). Remote patient monitoring: Information reliability challenges. *2009 9th International Conference on Telecommunication in Modern Satellite, Cable, and Broadcasting Services*, 295–301. https://doi.org/10.1109/TELSKS.2009.5339520

Rahmatinia, S., & Fahimi, B. (2017). Magneto-Thermal Modeling of Biological Tissues: A Step Toward Breast Cancer Detection. *IEEE Transactions on Magnetics*, *53*(6), 1–4. https://doi.org/10.1109/TMAG.2017.2671780

Ramesh, M. V, Anand, S., & Rekha, P. (2012). A mobile software for health professionals to monitor remote patients. *2012 Ninth International Conference on Wireless and Optical Communications Networks (WOCN)*, 1–4. https://doi.org/10.1109/WOCN.2012.6335565

Razaz, M. A., Algaolahi, A. Q., Makarem, M. A., & Alwardy, E. H. (2024). VLC Channel estimation for indoor environment using LSTM. *2024 4th International Conference on Emerging Smart Technologies and Applications (ESmarTA)*, 1–4. https://doi.org/10.1109/eSmarTA62850.2024.10638984

Saeedkia, D., Mansour, R. R., & Safavi-Naeini, S. (2005). Analysis and design of a continuous-wave terahertz photoconductive photomixer array source. *IEEE Transactions on Antennas and Propagation*, *53*(12), 4044–4050. https://doi.org/10.1109/TAP.2005.859909

Sagahyroon, A. (2017). Remote patients monitoring: Challenges. *2017 IEEE 7th Annual Computing and Communication Workshop and Conference (CCWC)*, 1–4. https://doi.org/10.1109/CCWC.2017.7868460

Sakamoto, T., & Koda, T. (2020). Respiratory Motion Imaging Using 2.4-GHz Nine-Element-Array Continuous-Wave Radar. *IEEE Microwave and Wireless Components Letters*, *30*(7), 717–720. https://doi.org/10.1109/LMWC.2020.2992541

Salama, W. M., Aly, M. H., & Amer, E. S. (2023). Deep learning based channel estimation optimization in VLC systems. *Optical and Quantum Electronics*, *55*(1), 79.

SalmanOgli, A., & Rostami, A. (2013). Plasmon Modes Hybridization Influence on Nano-Bio-Sensors Specification. *IEEE Transactions on Nanotechnology*, *12*(5), 858–866. https://doi.org/10.1109/TNANO.2013.2277760

Saxena, A. K., Dixit, R. R., & Aman-Ullah, A. (2022). An LSTM Neural Network Approach to Resource Allocation in Hospital Management Systems. *International Journal of Applied Health Care Analytics*, *7*(2), 1–12. https://norislab.com/index.php/IJAHA/article/view/69

Saxena, V. N., Dwivedi, V. K., & Gupta, J. (2023). Machine Learning in Visible Light Communication System: A Survey. *Wireless Communications and Mobile Computing*, *2023*(1), 3950657. https://doi.org/https://doi.org/10.1155/2023/3950657

Sayem, A. S. Md., Simorangkir, R. B. V. B., Esselle, K. P., & Hashmi, R. M. (2019). Development of Robust Transparent Conformal Antennas Based on Conductive Mesh-Polymer Composite for Unobtrusive Wearable Applications. *IEEE Transactions on Antennas and Propagation*, *67*(12), 7216–7224. https://doi.org/10.1109/TAP.2019.2930116

Schmalz, K., Rothbart, N., Neumaier, P. F.-X., Borngräber, J., Hübers, H.-W., & Kissinger, D. (2017). Gas Spectroscopy System for Breath Analysis at mm-wave/THz Using SiGe BiCMOS Circuits. *IEEE Transactions on Microwave*

Theory and Techniques, *65*(5), 1807–1818. https://doi.org/10.1109/TMTT.2017.2650915

Shah, S. S., Safa, A., Johal, K., Obika, D., & Valentine, S. (2021). A prospective observational real world feasibility study assessing the role of app-based remote patient monitoring in reducing primary care clinician workload during the COVID pandemic. *BMC Family Practice*, *22*(1), 1–9.

Shang, J., & Yu, Y. (2019). An Ultrawideband Capsule Antenna for Biomedical Applications. *IEEE Antennas and Wireless Propagation Letters*, *18*(12), 2548–2551. https://doi.org/10.1109/LAWP.2019.2942842

Sharma, A., Keshari, P., & Bhatia, V. (2023). LSTM-based Channel Estimator for Optical IRS-Assisted non-Linear VLC Systems. *2023 IEEE International Conference on Advanced Networks and Telecommunications Systems (ANTS)*, 114–119. https://doi.org/10.1109/ANTS59832.2023.10468699

Shoaib, Z., Kamran, M. A., Mannan, M. M. N., & Jeong, M. Y. (2019). Methodologies on the Enhanced Spatial Resolution of Non-Invasive Optical Brain Imaging: A Review. *IEEE Access*, *7*, 130044–130066. https://doi.org/10.1109/ACCESS.2019.2939475

Shu, Y.-H., Chang, Y.-H., Lin, Y.-Z., & Chow, C.-W. (2024). Real-Time Indoor Visible Light Positioning (VLP) Using Long Short Term Memory Neural Network (LSTM-NN) with Principal Component Analysis (PCA). *Sensors*, *24*(16). https://doi.org/10.3390/s24165424

Subramaniam, E. V. D., Srinivasan, K., Qaisar, S. M., & Pławiak, P. (2023). Interoperable IoMT Approach for Remote Diagnosis with Privacy-Preservation Perspective in Edge Systems. *Sensors*, *23*(17). https://doi.org/10.3390/s23177474

Ullah, A., Choi, W., & Coleri, S. (2023). Path Loss Estimation and Jamming Detection in Hybrid RF-VLC Vehicular Networks: A Machine-Learning Framework. *IEEE Sensors Journal*, *23*(24), 31325–31336. https://doi.org/10.1109/JSEN.2023.3329490

Usman, M., Asghar, M. R., Ansari, I. S., & Qaraqe, M. (2018). Security in Wireless Body Area Networks: From In-Body to Off-Body Communications. *IEEE Access*, *6*, 58064–58074. https://doi.org/10.1109/ACCESS.2018.2873825

Van Houdt, G., Mosquera, C., & Nápoles, G. (2020). A review on the long short-term memory model. *Artificial Intelligence Review*, *53*(8), 5929–5955.

Wang, X., Zhao, Q., Xi, R., Li, C., Li, G., & Li, L. (2021). Review of Bridge Structural Health Monitoring Based on GNSS: From Displacement Monitoring to Dynamic Characteristic Identification. *IEEE Access*, *9*, 80043–80065. https://doi.org/10.1109/ACCESS.2021.3083749

Xiao, H., Tian, W., Liu, W., & Shen, J. (2022). ChannelGAN: Deep Learning-Based Channel Modeling and Generating. *IEEE Wireless Communications Letters*, *11*(3), 650–654. https://doi.org/10.1109/LWC.2021.3140102

Xu, L.-J., Chu, Z.-J., Zhu, L., Xu, J.-P., & Duan, Z. (2021). Design and Analysis of Dual-Band Implantable Antennas Based on Effective Relative Permittivity Calculation. *IEEE Transactions on Antennas and Propagation*, *69*(5), 2463–2472. https://doi.org/10.1109/TAP.2020.3030958

Xu, L.-J., Jin, X., Hua, D., Lu, W.-J., & Duan, Z. (2020). Realization of Circular Polarization and Gain Enhancement for Implantable Antenna. *IEEE Access*, *8*, 16857–16864. https://doi.org/10.1109/ACCESS.2019.2963744

Xu, L.-J., Xu, J.-P., Chu, Z.-J., Liu, S., & Zhu, X. (2020). Circularly Polarized Implantable Antenna With Improved Impedance Matching. *IEEE Antennas and Wireless Propagation Letters*, *19*(5), 876–880. https://doi.org/10.1109/LAWP.2020.2983216

Yakovlev, A., Kim, S., & Poon, A. (2012). Implantable biomedical devices: Wireless powering and communication. *IEEE Communications Magazine*, *50*(4), 152–159. https://doi.org/10.1109/MCOM.2012.6178849

Yan, D., Li, X., Ma, C., Qiu, G., Cao, M., Li, J., & Guo, S. (2022). Terahertz Refractive Index Sensing Based on Gradient Metasurface Coupled Confined

Spoof Surface Plasmon Polaritons Mode. *IEEE Sensors Journal*, *22*(1), 324–329. https://doi.org/10.1109/JSEN.2021.3130266

Yang, P., Xiao, Y., Xiao, M., & Li, S. (2019). 6G Wireless Communications: Vision and Potential Techniques. *IEEE Network*, *33*(4), 70–75. https://doi.org/10.1109/MNET.2019.1800418

Zakerabasali, S., & Ayyoubzadeh, S. (2022). Internet of Things and healthcare system: A systematic review of ethical issues. *Health Science Reports*, *5*. https://doi.org/10.1002/hsr2.863

Zengeya, T., & Vincent Fonou-Dombeu, J. (2024). A Review of State of the Art Deep Learning Models for Ontology Construction. *IEEE Access*, *12*, 82354–82383. https://doi.org/10.1109/ACCESS.2024.3406426

Zerrad, F., Taouzari, M., Makroum, E. M., Aoufi, J. El, Qanadli, S. D., Karaaslan, M., Al-Gburi, A. J. A., & Zakaria, Z. (2023). Microwave Imaging Approach for Breast Cancer Detection Using a Tapered Slot Antenna Loaded with Parasitic Components. *Materials*, *16*(4). https://doi.org/10.3390/ma16041496

Zhang, S. (2022). Challenges in KNN Classification. *IEEE Transactions on Knowledge and Data Engineering*, *34*(10), 4663–4675. https://doi.org/10.1109/TKDE.2021.3049250

Zhao, S., Wang, H., Li, Y., Nie, L., Zhang, S., Xing, D., & Qin, H. (2022). Ultrashort-Pulse-Microwave Excited Whole-Breast Thermoacoustic Imaging With Uniform Field of Large Size Aperture Antenna for Tumor Screening. *IEEE Transactions on Biomedical Engineering*, *69*(2), 725–733. https://doi.org/10.1109/TBME.2021.3104137

Zhu, X., Wang, C.-X., Huang, J., Chen, M., & Haas, H. (2022). A Novel 3D Non-Stationary Channel Model for 6G Indoor Visible Light Communication Systems. *IEEE Transactions on Wireless Communications*, *21*(10), 8292–8307. https://doi.org/10.1109/TWC.2022.3165569

Zwaag, K. M. Van Der, Marinho, M. P., Costa, W. D. S., De Assis Souza Dos Santos, F., Bastos-Filho, T. F., Rocha, H. R. O., Segatto, M. E. V, & Silva, J.

A. L. (2021). A Manchester-OOK Visible Light Communication System for Patient Monitoring in Intensive Care Units. *IEEE Access*, *9*, 104217–104226. https://doi.org/10.1109/ACCESS.2021.3099462

CURRICULUM VITAE